European Journal of Medicinal Chemistry 277 (2024) 116777

Contents lists available at ScienceDirect

European Journal of Medicinal Chemistry

journal homepage: www.elsevier.com/locate/ejmech

Research paper

# Synthesis and photo-induced anticancer activity of new 2-phenylethenyl-1*H*-benzo[*e*]indole dyes

Gabrielė Varvuolytė [a,b], Eva Řezníčková [c,*], Sonata Krikštolė [a], Rasa Tamulienė [b], Aurimas Bieliauskas [b], Lukáš Malina [d], Veronika Vojáčková [c], Zdenko Duben [c], Hana Kolářová [d], Neringa Kleizienė [b], Eglė Arbačiauskienė [a], Asta Žukauskaitė [e], Vladimír Kryštof [c,f], Algirdas Šačkus [a,b,**]

[a] Department of Organic Chemistry, Kaunas University of Technology, LT-50254, Kaunas, Lithuania
[b] Institute of Synthetic Chemistry, Kaunas University of Technology, LT-51423, Kaunas, Lithuania
[c] Department of Experimental Biology, Faculty of Science, Palacký University, CZ-77900, Olomouc, Czech Republic
[d] Department of Medical Biophysics, Faculty of Medicine and Dentistry, Palacký University, CZ-77515, Olomouc, Czech Republic
[e] Department of Chemical Biology, Faculty of Science, Palacký University, CZ-77900, Olomouc, Czech Republic
[f] Institute of Molecular and Translational Medicine, Faculty of Medicine and Dentistry, Palacký University, CZ-77900, Olomouc, Czech Republic

ARTICLE INFO

*Keywords:*
DNA damage
Knoevenagel condensation
benzo[*e*]indole
photo-induced activity
reactive oxygen species

ABSTRACT

Herein, a series of new 1,1,2-trimethyl-1*H*-benzo[*e*]indole dyes was prepared *via* Knoevenagel condensation reaction between 1,1,2-trimethyl-1*H*-benzo[*e*]indole and benzaldehydes, and characterized using various spectroscopic methods. The obtained compounds showed cytotoxic properties in G361 melanoma cell line upon irradiation with 414 nm blue light at submicromolar doses. The mechanism of action of the most potent compound **15** was further investigated. The treatment induced substantial generation of reactive oxygen species, leading to DNA damage followed by cell death depending on the concentration of the photosensitizer compound and the irradiation intensity.

## 1. Introduction

1,1,2-Trimethyl-1*H*-benzo[*e*]indole has emerged as a versatile building block with numerous applications in biomedical and technical fields. It can be readily *N*-alkylated to yield benzo[*e*]indolium salts as valuable synthons for the preparation of dyes [1]. Over the years, benzo[*e*]indolium dyes have been extensively investigated, revealing numerous potential practical applications, for instance, in materials science [2,3]. Benzo[*e*]indolium dyes with possible applications in biology are of particular interest (Fig. 1). For example, compound **i** has emerged as a potential self-assembling, turn-on fluorescent probe for the selective detection of serum albumin [4]. Benzo[*e*]indolium dye **ii** has been examined as a highly selective turn-on fluorescent probe for toxic cyanide anions *via* the nucleophilic addition of cyanide to the positively charged benzo[*e*]indole moiety [5]. On the other hand, detection of sulfur dioxide derivatives in aqueous solutions and live cells occurs through the sulfite addition to the ethylenic double bond in the benzoindolium dyes [6]. Moreover, *N*-alkylated benzo[*e*]indolium dyes preferentially localize in the cell mitochondria, making the cationic benzo[*e*]indolium a mitochondrion-targeting fragment [7]. The benzoindolium-aniline derivative **iii** has been used to monitor abnormal mitochondrial viscosity, due to its rotatable C–C bond [8]. Noteworthy, mitochondria-specific benzoindolium dyes have been reported as probes for detecting and imaging cysteine, (bi)sulfite, hypochlorite ions, or as anticancer agents with significant cytotoxicity in vitro [9–13]. The mitochondrion is also an important source of reactive oxygen species (ROS), which can cause mitochondrial membrane depolarization and cell death. Thus, the development of new mitochondria-localized photosensitizers for photodynamic anticancer therapy is of great importance [14]. The most extensively studied benzo[*e*]indole-derived photosensitizer is the *N*-sulfobutylated benzo[*e*]indolium dye indocyanine green [15,16]. Recently, several other promising near-infrared benzo[*e*]indolium-based photosensitizers for photodynamic/photothermal therapy have also been reported [17–20].

* Corresponding author. Department of Experimental Biology, Faculty of Science, Palacký University, Šlechtitelů 27, CZ-77900, Olomouc, Czech Republic.
** Corresponding author. Institute of Synthetic Chemistry, Kaunas University of Technology, K. Baršausko g. 59, LT-51423, Kaunas, Lithuania.
*E-mail addresses:* eva.reznickova@upol.cz (E. Řezníčková), algirdas.sackus@ktu.lt (A. Šačkus).

https://doi.org/10.1016/j.ejmech.2024.116777
Received 2 July 2024; Received in revised form 9 August 2024; Accepted 12 August 2024
Available online 13 August 2024

On the other hand, relatively scarce examples of benzo[*e*]indole non-*N*-alkylated counterparts **iv-viii** and their possible uses have been reported. Depending on the pH in the surrounding environment, the benzo[*e*]indole nitrogen atom can be either protonated or deprotonated. In its protonated (acidic) form, the dye exhibits intense fluorescence, whereas the basic deprotonated form is non-fluorescent. Therefore, benzo[*e*]indoles **iv-viii** have been revealed to accumulate in acidic cell organelles (e.g. lysosomes), ratiometrically monitor pH fluctuations, or changes of metal ion concentrations in living cells [21–26].

To the best of our knowledge, the photocytotoxic properties of the non-alkylated phenylethenylbenzo[*e*]indoles remain largely unexplored. To bridge this gap, in the present work we ought to synthesize a series of small-molecule phenylethenylbenzo[*e*]indoles containing various electron-donating and/or electron-withdrawing groups and to evaluate their photocytotoxic activity in skin melanoma cells.

## 2. Results and discussion

### 2.1. Chemistry

The Knoevenagel and Knoevenagel-like condensation reactions, which occur between active methylene groups and aldehydes, remain an easy and atom-efficient way to construct new C=C bonds, and hence have been successfully applied to synthesize biologically relevant compounds and dyestuffs [27]. Throughout the years, the Knoevenagel-type condensation has been employed to obtain new (benzo)indolium dyes with practical applications in biology. The Knoevenagel reaction is carried out in the presence of secondary amines, such as piperidine [28,29], or tertiary amines like triethylamine [30–32], typically in ethanol as the solvent of choice, affording indolium and benzoindolium dyes in good yields. On the other hand, the use of acids in the synthesis of (benzo)indolium derivatives through the Knoevenagel-like condensation reaction, for example, acetic anhydride [8,33], acetic acid [34] or a mixture thereof [35], acetic acid or trifluoroacetic acid in ethanol [36,37], and the use of piperidine along with acetic acid in ethanol [38] were reported as well.

In this work, Knoevenagel-type reaction was employed to prepare a small library of 2-phenylethenyl-1*H*-benzo[*e*]indoles starting from commercially available 1,1,2-trimethyl-1*H*-benzo[*e*]indole **1** and variously substituted benzaldehydes. The initial optimization of reaction conditions was started with compound **1** and benzaldehyde as model substrates (see Table 1).

When the reaction was performed in the presence of piperidine in ethanol at reflux for 24 h, no product was detected (Table 1, Entry 1). The microwave-assisted heating also failed to yield positive results (Table 1, Entry 2). Nevertheless, while following the addition of acetic acid to the reaction mixture and refluxing for 24 h, the desired product **2** was successfully isolated in a high yield of 83 % (Table 1, Entry 3). In this case, microwave-assisted heating did not improve the yield of the product (Table 1, Entry 4).

Additionally, when the Knoevenagel-like condensation reaction of benzo[*e*]indole **1** and benzaldehyde was carried out in acetic acid in the presence of acetic anhydride, only 20 % yield was reached after 2 h (Table 1, Entry 5). Extending the reaction time to 24 h resulted in the formation of unidentified side products and substantial decrease in the amount of the desired product. The use of trifluoroacetic acid was detrimental to the reaction yield as well (Table 1, Entry 6).

Thus, the reaction conditions using piperidine and acetic acid in ethanol as the solvent at reflux were chosen for the synthesis of the compounds. Using this method, compounds **2**–**21** were successfully synthesized from 1,1,2-trimethyl-1*H*-benzo[*e*]indole **1** and various benzaldehydes, in yields ranging from 16 % to 95 % (Scheme 1).

Substituent effects on the yield could also be observed, for example, excellent yields were reached with benzaldehydes containing electron-withdrawing 3-nitro, 4-cyano, and 3-trifluoromethyl groups. In these cases, compounds **8**, **10** and **13** were obtained with yields of 82 %, 95 %, and 85 %, respectively. Compounds **4** and **5**, containing electron-donating dimethyl- and diethylamino groups in the 4-position, were obtained in relatively low yields of 21 % and 16 % respectively, when the piperidine/acetic acid in ethanol system was used. Stirring the reaction mixture in acetic acid resulted in traces of the product. However, conducting the reaction in ethanol, and in the presence of trifluoroacetic acid improved the yields of the target benzo[*e*]indoles **4** and **5** to 31 % and 55 %, respectively (Scheme 1).

It should be noted that the reaction of benzo[*e*]indole **1** with 4-fluoro-3-nitrobenzaldehyde in piperidine/acetic acid and ethanol yielded

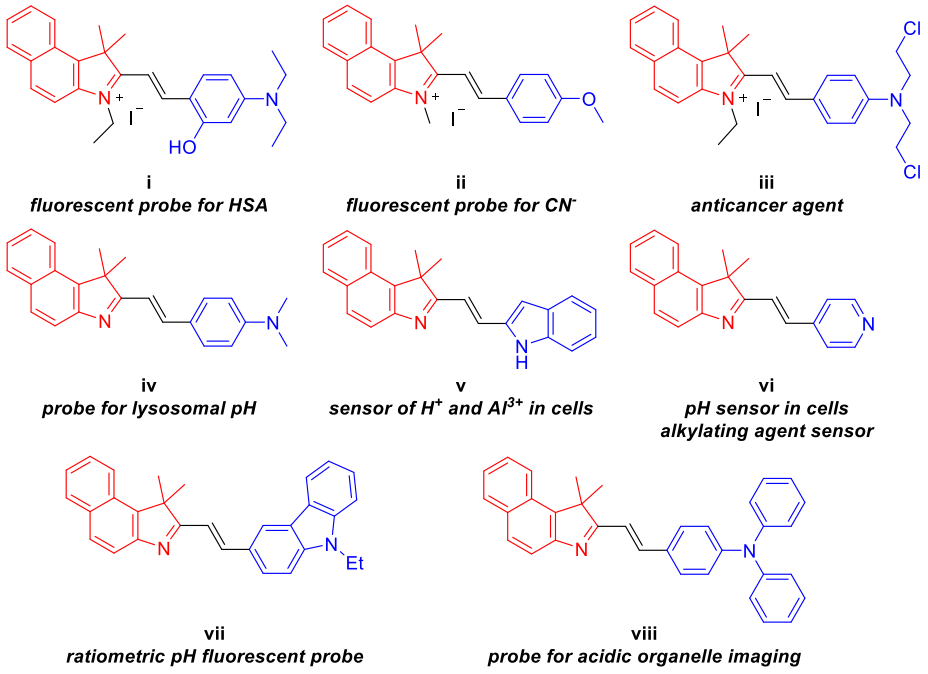


**Fig. 1.** Examples of benzo[*e*]indole derivatives.

**Table 1**
Optimization of the Knoevenagel reaction conditions using compound **1** and benzaldehyde as a model system.

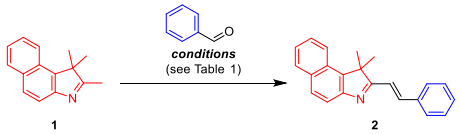


| Entry | Base | Acid | Solvent | Heating | Temperature | Yield (%) |
|---|---|---|---|---|---|---|
| 1 | piperidine | – | EtOH | conventional | reflux | 0 |
| 2 | piperidine | – | EtOH | MW-assisted | 85 °C | 0 |
| **3** | **piperidine** | **AcOH** | **EtOH** | **conventional** | **reflux** | **83** |
| 4 | piperidine | AcOH | EtOH | MW-assisted | 85 °C | 45 |
| 5 | – | $Ac_2O$, AcOH | | conventional | 90 °C | 20 |
| 6 | – | TFA | EtOH | conventional | reflux | 21 |

only a side product with a molecular weight of 234 g/mol. According to the $^1$H NMR spectrum, it was determined that 3-nitro-4-(piperidin-1-yl) benzaldehyde was formed, most likely, upon the replacement of the fluorine atom in the benzaldehyde molecule with piperidine through a competing $S_NAr$ reaction (Scheme S1). Electron-withdrawing groups situated at 2- or 4-position to the substitution site are known to increase the rate of $S_NAr$ reaction [39]. Thus, to synthesize the desired benzo[*e*] indole derivative **22**, triethylamine was used, as it should not participate in the undesired $S_NAr$ reaction with the fluorine leaving group. The compound **22** was thus successfully obtained in a satisfactory yield of 55 % (Scheme 1).

Structures of all the compounds **2**–**22** were confirmed by NMR, FT-IR, HRMS data. In the FT-IR spectra of the compounds **7**–**11**, **15**–**18**, **20**–**22**, characteristic nitrile C≡N stretching bands appear at 2224-2238 cm$^{-1}$, asymmetrical $NO_2$ bands – in the range of 1509–1533 cm$^{-1}$, symmetrical – at 1336-1348 cm$^{-1}$.

The structures of compounds **2**–**22** were elucidated using a combination of standard and advanced NMR spectroscopy techniques, i.e. $^{13}$C DEPT-90, $^{13}$C DEPT-135, $^1$H–$^1$H COSY, $^1$H–$^1$H TOCSY, $^1$H–$^1$H NOESY, $^1$H–$^{13}$C HSQC, $^1$H–$^{13}$C HMBC, $^1$H–$^{13}$C H2BC, $^1$H–$^{15}$N HMBC, and 1,1-ADEQUATE, where the compound **15** was subjected to an in-depth NMR analysis (Fig. 2). The aforementioned phenylethenyl compounds contain a benzo[*e*]indole moiety connected to aryl groups *via* an ethene bridge. The *E*-configuration of the ethene double bond unequivocally follows from the magnitude of the vicinal coupling between the olefinic protons $H_a$ ($\delta$ 6.90−7.28 ppm) and $H_b$ ($\delta$ 7.78−8.17 ppm), which exhibited an AB-spin system and appeared as two sets of doublets ($^3J_{Ha,Hb}$ = 16.0−16.5 Hz). The distinction between ethene bridge protons and other distinct $^1$H spin systems was mainly made from the $^1$H–$^1$H NOESY, $^1$H–$^{15}$N HMBC, and $^1$H–$^{13}$C HMBC spectral data.

For instance, in the $^1$H NMR spectrum of compound **15**, the well-resolved six-proton singlet ($\delta$ 1.69 ppm) was easily attributed to the geminal methyl groups at C-1 from the benzo[*e*]indole moiety. Moreover, the $^1$H–$^1$H NOESY spectrum revealed strong NOEs between the protons of geminal methyl groups ($\delta$ 1.69 ppm) and the 9-H ($\delta$ 8.06 ppm), olefinic $H_a$ ($\delta$ 7.07 ppm) protons, confirming their proximity in space. Furthermore, a comparison between the $^1$H–$^1$H COSY and $^1$H–$^1$H TOCSY spectra confirmed these assignments, as the 9-H proton belonged to a four-proton spin system. As expected, the olefinic $H_a$ proton had only a two-proton spin system, where the olefinic $H_b$ proton resonated at $\delta$ 7.79 ppm ($^3J_{Ha,Hb}$ = 16.2 Hz). The chemical shifts of olefinic carbons $CH_a$ ($\delta$ 119.6 ppm) and $CH_b$ ($\delta$ 134.4 ppm) were easily deduced from the $^1$H–$^{13}$C HSQC spectrum. Then, with the addition of 1,1-ADEQUATE spectral data, this information confirmed that the protonated $CH_a$ carbon was adjacent to the indole quaternary carbon C-2 ($\delta$ 184.4 ppm). At the same time, the $CH_b$ carbon correlated with the adjacent quaternary carbon C-1′ ($\delta$ 129.0 ppm) from the 4-methoxy-3-nitrophenyl moiety. Finally, long-range $^1$H–$^{13}$C HMBC, $^1$H–$^{15}$N HMBC, and $^1$H–$^{13}$C H2BC correlations further confirmed the chemical shift assignments, thus allowing different structural fragments to be joined.

The $^{19}$F NMR spectra of benzo[*e*]indole derivatives **12**–**14**, **18**–**20**, **22** showed that the chemical shifts for various fluorophenyl-substituted derivatives ranged from $\delta$ −106.1 to −116.5 ppm. In comparison, trifluoromethylphenyl-substituted compounds resonated from $\delta$ −62.7 to −63.0 ppm, which is in good agreement with the data in the literature [40].

To determine the wavelength of light, at which our benzo[*e*]indole derivatives **2**–**22** should be irradiated for the investigation of their photo-induced activity, their absorption and fluorescence properties were measured in aqueous solutions. All of the compounds, except **4** and **5**, had two intense absorption bands, with the high energy band in the 280–320 nm range, and low energy bands at longer wavelengths, in the visible light spectrum (Fig. S1, Table S1). Compared to compound **2**, which possesses an unsubstituted phenyl ring, the introduction of electron-donating substituents induced a bathochromic shift of the absorption maxima, while electron-withdrawing substituents to some extent blue-shifted the $\lambda_{max}$. Notably, compound **5**, which contains a 4-diethylamino group, had the most red-shifted absorption maximum, at 457 nm. It is known that the nitro group can be a fluorescence quencher, depending on its position, and the surrounding substituents in the molecule [41–44]. In the case of our compounds, weaker fluorescence was observed for nitro group bearing compounds **8**, **9**, **15**, **17**, **22**, having nitro groups in the 2- or 3-position of the phenyl ring.

### 2.2. Biology

Although the compounds exhibited the ability to absorb both UV and visible blue light, because of the harmful effects of UV and near-UV light on cells [45], we chose a 414 nm emitting LED source for conducting the experiments [46]. To evaluate the photo-inducible effects of the synthesized compounds, G361 cells were treated with the compounds for 4 h and then exposed to blue light, with a total irradiation dose of 10 J/cm$^2$. Cell viability was measured 72 h after irradiation using an MTT assay [47], which demonstrated photocytotoxic properties of the compounds. The structure-activity relationship analysis revealed several key insights into the potency of the compounds. With the exception of the 4-dimethylamino and 4-diethylamino substituted compounds **4** and **5**, respectively, all other compounds displayed cytotoxicity at low micromolar and submicromolar concentrations (Table 2). Notably, lower cytotoxicity of the compounds was observed in the dark. Upon light irradiation, the cytotoxicity of the unsubstituted derivative **2** increased by only 2-fold. On the other hand, 3-nitro (compounds **8**, **15**, **16**, **17**) and 4-cyano substituted derivatives (compounds **10**, **18**) exhibited the highest photo-induced cytotoxicity with submicromolar $EC_{50}$ values, whereas their activity in the dark was 7–28 times lower. Among these, 4-methoxy-3-nitro and 4-chloro-3-nitro substituted compounds **15** and **17**, respectively, were the most potent. In this case, the 4-methoxy and 4-chloro substituents substantially enhanced the potency of 3-nitro

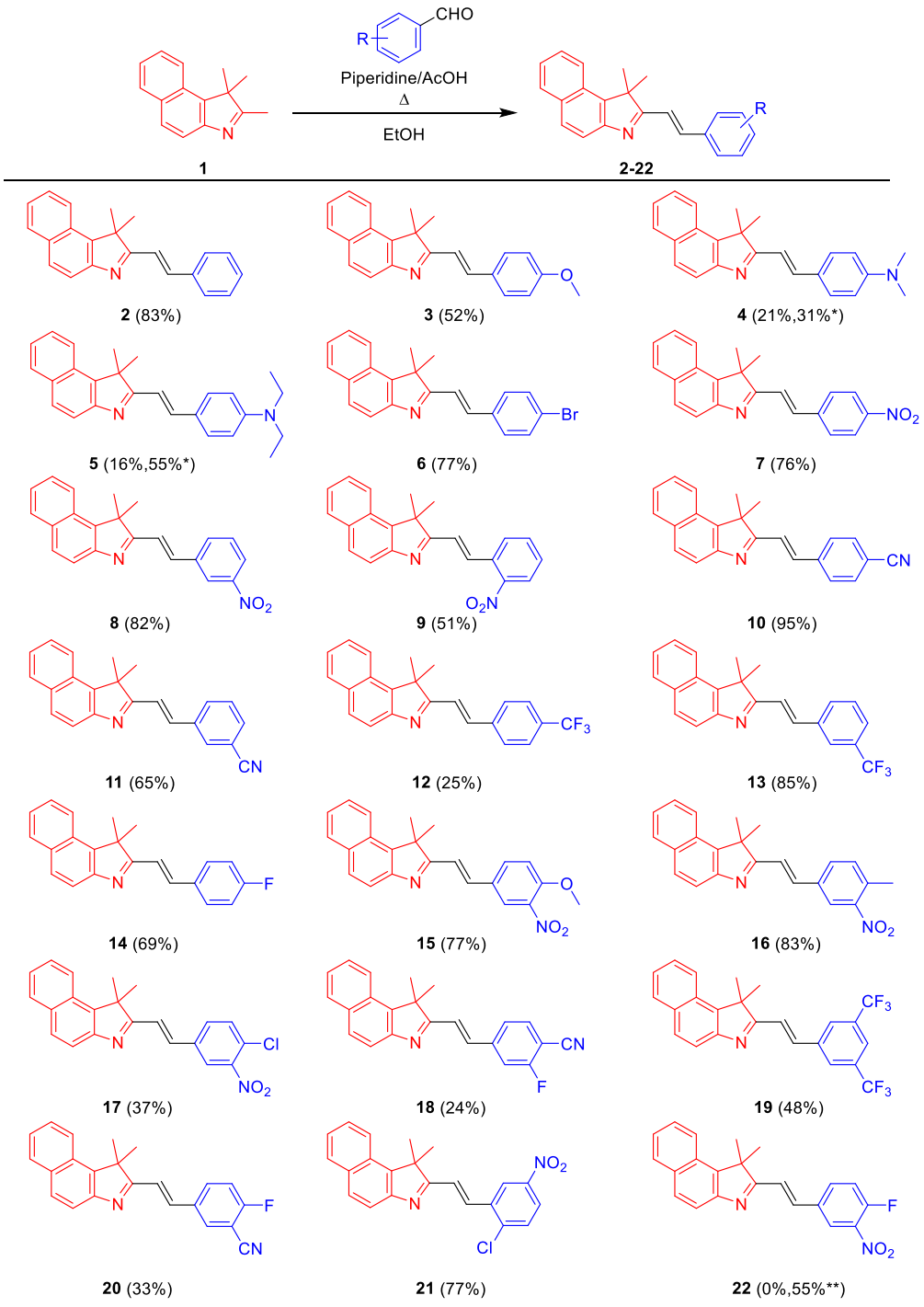


**Scheme 1.** Synthesis of compounds **2**–**22**. Alternative reaction conditions: *TFA, EtOH, reflux, 24 h; **TEA, EtOH, reflux, 24 h.

substituted compound **8**, whereas the introduction of other substituents was less favourable (compounds **16**, **21**, **22**). Moreover, the trifluoromethyl substituted derivatives **12**, **13**, and **19** were also more potent than the unsubstituted derivative **2**, with the 3,5-bis(trifluoromethyl) derivative **19** outperforming its 3-(trifluoromethyl) substituted counterpart **13** and the 4-(trifluoromethyl) isomer **12**. Interestingly, the 2-chloro-5-nitro substituted compound **21** was less potent, contrary to the high potency of the 4-chloro-3-nitro substituted derivative **17**.

Compounds possessing a selectivity ratio greater than 5 between dark and light-induced cytotoxicity in G361 melanoma cells were selected as possible candidates for further evaluation. The dark cytotoxicity of these compounds was evaluated in confluent normal human fibroblasts BJ, a model of non-transformed cells with low proliferation potential that allows to mimic surrounding healthy tissue which is affected by the compound but is not irradiated by light (Table 2). The tested compounds exhibited comparable or elevated $EC_{50}$ values in BJ cells compared to non-irradiated G361 melanoma cells.

Compound **15** was the most potent and showed almost 30-fold higher potency in the G361 cell line after blue light irradiation than in the dark. The dark cytotoxicity of compound **15** was found to be even more reduced in confluent BJ cells (8.3 μM), exhibiting a more favourable selectivity ratio (>40 times) when compared to the $EC_{50}$ value obtained for G361 cells after irradiation. Compound **15** was therefore

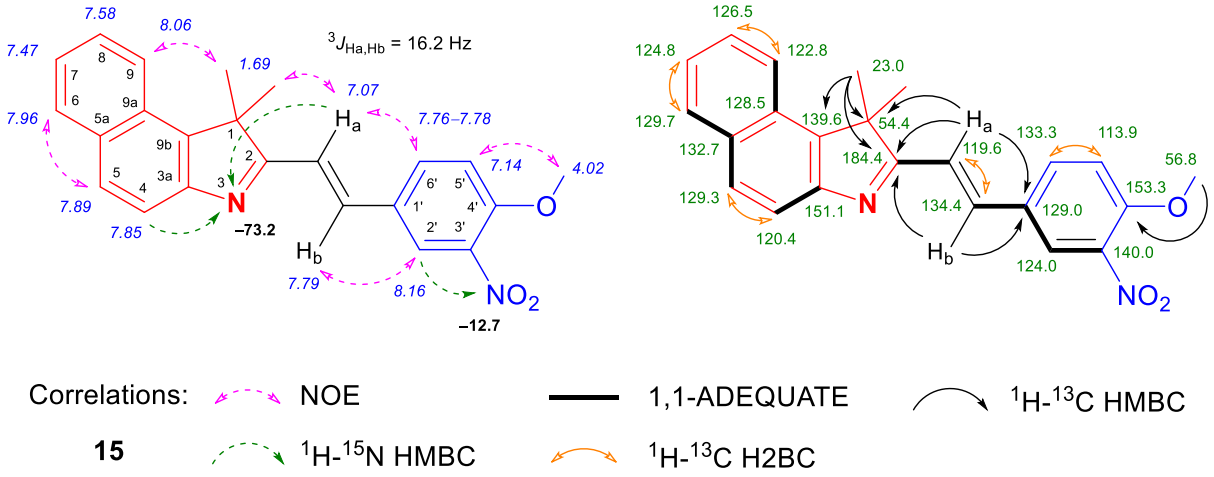


**Fig. 2.** Relevant $^1$H–$^1$H NOESY, $^1$H–$^{15}$N HMBC, 1,1-ADEQUATE, $^1$H–$^{13}$C HMBC, and $^1$H–$^{13}$C H2BC correlations, as well as $^1$H NMR (italics), $^{13}$C NMR, and $^{15}$N NMR (bold) chemical shifts of compound **15**.

**Table 2**
Cytotoxicity of compounds **2**–**22** in G361 and BJ cells.

| Cmpd. | $EC_{50}$ ± SD (μM) | | |
|---|---|---|---|
| | G361 | | BJ |
| | Dark | Light (414 nm, 10 J/cm$^2$) | Dark |
| **2** | 6.5 ± 1.0 | 2.8 ± 1.1 | n.d. |
| **3** | 9.5 ± 0.6 | 5.2 ± 1.0 | n.d. |
| **4** | >10 | >10 | n.d. |
| **5** | >10 | >10 | n.d. |
| **6** | 7.6 ± 2.2 | 1.3 ± 0.2 | >10 |
| **7** | 5.7 ± 3.2 | 0.8 ± 0.5 | 6.0 ± 0.2 |
| **8** | 2.9 ± 1.3 | 0.4 ± 0.3 | 5.0 ± 0.7 |
| **9** | 7.8 ± 0.4 | 1.1 ± 0.2 | >10 |
| **10** | 5.1 ± 1.2 | 0.5 ± 0.1 | 6.7 ± 1.5 |
| **11** | 3.7 ± 0.2 | 0.9 ± 0.4 | n.d. |
| **12** | 4.0 ± 0.7 | 0.9 ± 0.8 | n.d. |
| **13** | 7.6 ± 0.3 | 1.3 ± 0.0 | >10 |
| **14** | 7.3 ± 0.8 | 4.1 ± 0.8 | n.d. |
| **15** | 5.6 ± 0.5 | 0.2 ± 0.0 | 8.3 ± 0.8 |
| **16** | 6.6 ± 0.8 | 0.9 ± 0.6 | 8.0 ± 0.8 |
| **17** | 7.2 ± 2.4 | 0.3 ± 0.1 | >10 |
| **18** | 6.2 ± 0.6 | 0.6 ± 0.0 | 7.2 ± 1.2 |
| **19** | >10 | 1.3 ± 0.2 | >10 |
| **20** | 6.9 ± 2.5 | 1.4 ± 0.1 | n.d. |
| **21** | >10 | 7.9 ± 0.4 | n.d. |
| **22** | 7.9 ± 0.3 | 1.8 ± 0.5 | n.d. |

n.d. - not determined.

selected as the lead compound in the series. The evaluation of the photocytotoxicity induced by **15** was verified in another melanoma cell line, A375-derived ARN8 cells (Table 3). As with G361, **15** in combination with blue light (414 nm; 10 J/cm$^2$) also reduced the ARN8 cell viability in submicromolar concentrations. Although **15** showed low cytotoxicity in the dark in both cell lines tested, light exposure reduced the resulting $EC_{50}$ at least 15-fold after 24 h (9.0 vs 0.6 μM in G361 and 9.2 vs 0.5 μM in ARN8). This ratio was even higher when the cells were incubated for a longer period after irradiation (72 h; >28 times; Table 3). To further prove the link between the cytotoxicity of **15** and light irradiation, several light energy doses were applied after the treatment (Fig. 3). The experiment in both cell lines clearly revealed the dependency of the **15**-induced cytotoxicity on the light energy; each two-fold increase of energy reduced the resulting $EC_{50}$ value by approximately 1.7 times.

**Table 3**
Cytotoxicity of compound **15** in G361 and ARN8 melanoma cell lines.

| Cell line | Incubation | Cmpd. **15**: $EC_{50}$ ± SD (μM) | |
|---|---|---|---|
| | | Dark | Light (414 nm, 10 J/cm$^2$) |
| G361 | 24 h | 9.0 ± 1.4 | 0.6 ± 0.1 |
| | 72 h | 5.6 ± 0.5 | 0.2 ± 0.0 |
| ARN8 | 24 h | 9.2 ± 0.9 | 0.5 ± 0.1 |
| | 72 h | 7.3 ± 1.8 | 0.2 ± 0.1 |

Reactive oxygen species (ROS) generated by the photochemical reaction are often the main cause of the cytotoxicity of photo-inducible compounds [48]. To verify this phenomenon, ROS levels were measured in G361 and ARN8 cells using CM-$H_2$DCFDA probe, a general oxidative stress indicator, upon treatment with **15** immediately after the irradiation with blue light (414 nm) at two different energy levels (Fig. 4). In both cell lines tested, we observed a rapid increase in ROS levels that was concentration- as well as light energy dose-dependent, whereas in samples treated with **15** and kept in the dark, ROS levels remained unaltered. The ROS-inducing effect of **15** was attenuated by pretreatment with the ROS inhibitor *N*-acetylcysteine, which reduced the ROS induction by half. Similar efficacy was observed with recently reported indole-pyrazole derivatives [49] and also other structurally unrelated porphyrin photosensitizers [50,51].

In parallel, we used three other probes to further monitor the ROS formation in **15**-treated melanoma cells after blue light irradiation. We used another general oxidative stress indicator DHR123, the hydroxyl radical indicator HPF and the singlet oxygen sensor SOSG (Fig. S2). DHR123 probe signal fully correlated with the previously obtained results. While hydroxyl radical production was increased by **15** in combination with blue light irradiation, with a more pronounced effect in G361 cells compared to ARN8 cells, singlet oxygen levels were not significantly affected (Figs. S2A and B). ROS formation was confirmed also in DHR123 and HPF-containing aqueous solutions (i.e. without cells and medium) of **15** in combination with an irradiation dose of 10 J/cm$^2$, while no significant increase in singlet oxygen generation was observed (Fig. S2C). It is therefore likely that compound **15** induces a photodynamic effect through a type I mechanism, as it does not produce singlet oxygen [52]. In addition, we propose that the generation of ROS is the primary mechanism underlying photocytotoxic activity, a concept also suggested for related indole-pyrazole hybrids reported recently [49].

In response to oxidative stress, cells activate protective mechanisms, including the upregulation of heme oxygenase-1 (HO-1) [53]. The increased levels of HO-1 were observed in the immunoblotting analyses (Fig. 5) providing independent evidence of oxidative stress induced by **15** as initially detected in the fluorescence-based assay (Fig. 4). Elevated HO-1 levels in the sample treated with **15** without irradiation indicate

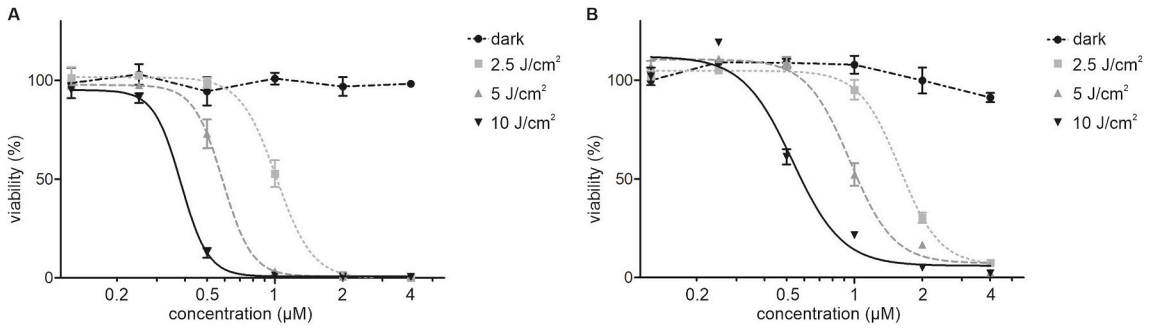


**Fig. 3.** Cytotoxicity of compound **15** is dependent on the intensity of blue light (414 nm) in G361 (**A**) and ARN8 (**B**).

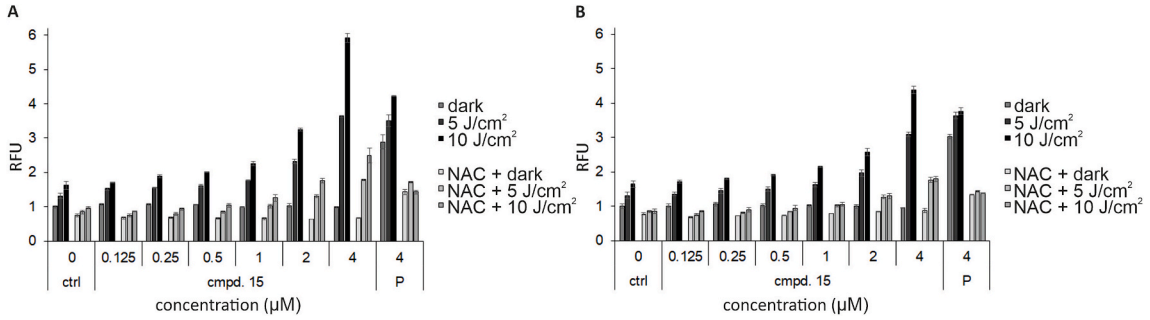


**Fig. 4.** Production of reactive oxygen species (ROS) in G361 (**A**) and ARN8 (**B**) cells treated with **15** and irradiated with indicated energy doses of blue light in the absence/presence of *N*-acetylcysteine (NAC). Relative fluorescence units (RFU) were normalised to the untreated control sample kept in the dark. Pyocyanin (P) was used as a control at a concentration of 4 μM.

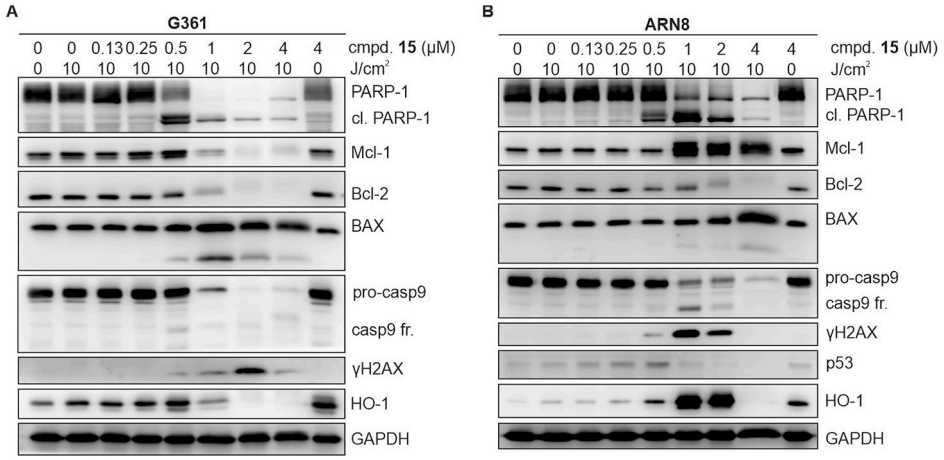


**Fig. 5.** Analysis of protein expression in G361 (**A**) and ARN8 (**B**) cells treated with **15** and exposed to blue light (414 nm, 10 J/cm$^2$). Cells were treated with **15** for 4 h, irradiated and then incubated for another 20 h. GAPDH was used as a control for equal protein loading.

ROS-mediated mild dark cytotoxicity of **15**. HO-1 induction was observed for various photosensitizers [49,54,55].

The primary consequence of increased ROS levels is the induction of cell death. In order to distinguish between the proapoptotic or pronecrotic effects of **15**, we analyzed several markers of apoptosis (Fig. 5). The cleavage of the protein PARP-1, which was observed in G361 cell line, together with the cleavage of procaspase 9, the disappearance of the antiapoptotic proteins Bcl-2 and Mcl-1 and, conversely, the increase and cleavage of the proapoptotic protein BAX, clearly indicates an apoptosis-inducing effect of **15** in this experimental setup. The same trend was also observed in the ARN8 cell line, with one exception: **15** in combination with blue light upregulated the level of Mcl-1 by a mechanism not elucidated in this study.

Compound **15**-induced apoptosis was further investigated in a follow-up experiment, where melanoma cells treated with two concentrations of **15** (0.5 and 1 μM) were irradiated with increasing doses of blue light (Fig. 6A,C) and was further confirmed by flow cytometry analysis (Fig. 6B,D). While in **15**-treated samples we observed a light energy dose-dependent enrichment of the cell population in the subG1 phase of the cell cycle, corresponding to the cells ongoing cell death, untreated and/or unirradiated samples were unaffected and the number of cells in the subG1 phase was insignificant. Although no significant alterations in cell cycle phase distribution were observed in G361 cells (Fig. S3), the induction of G2/M arrest was detected in ARN8 cells (Fig. S4) under several experimental conditions. This finding correlated with the appearance of elevated phosphorylation of H2AX at Ser139 (γH2AX), a known marker of DNA damage. Similar effects were observed with indole-pyrazole hybrids reported recently [49].

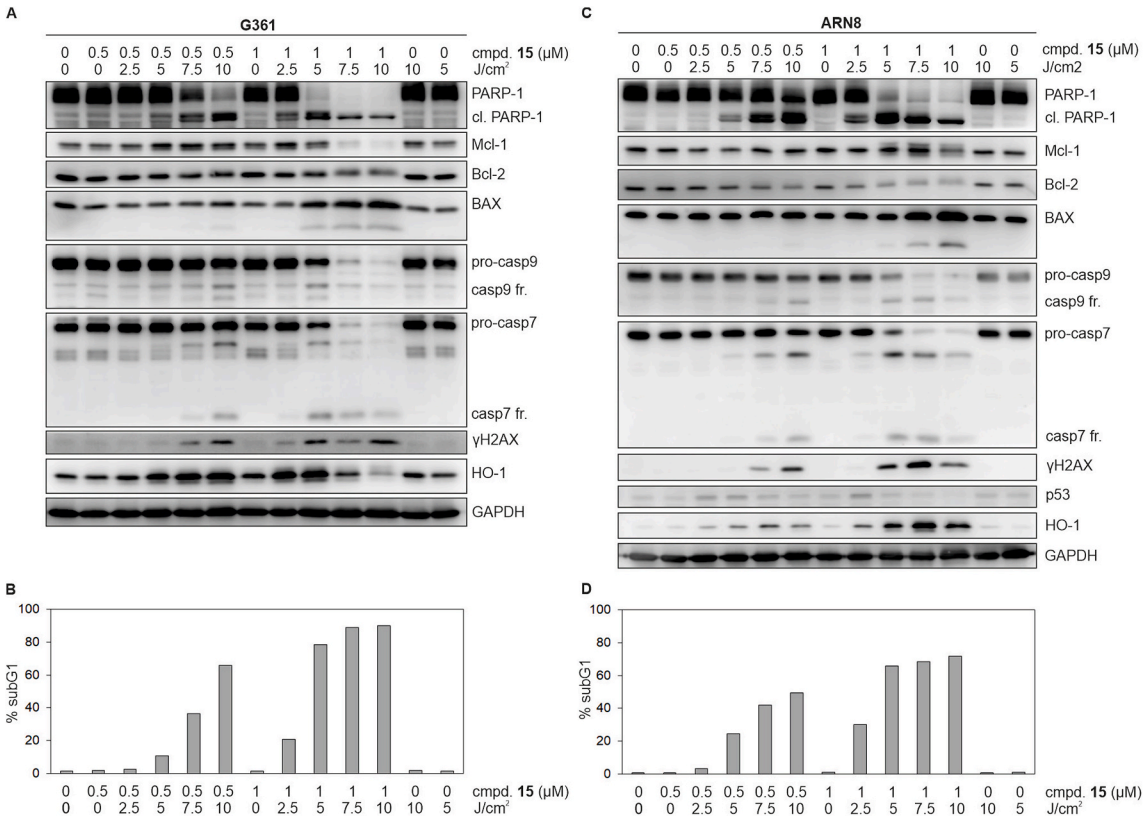


**Fig. 6.** Analysis of protein expression (**A**, **C**) and flow cytometry evaluation of subG1 population (**B**, **D**) in G361 (**A**, **B**) and ARN8 (**C**, **D**) cells treated with **15** and exposed to increasing energies of blue light (414 nm). Cells were treated with **15** for 4 h, irradiated and then incubated for another 20 h. GAPDH was used as a control for equal protein loading.

To independently confirm the extent of DNA damage induced by **15**, analysis of DNA fragmentation by the comet assay (Fig. 7), a method used for evaluation of DNA damage caused, amongst other, by different photosensitizers [56], was performed. While 0.5 μM **15** alone did not affect DNA integrity, in combination with irradiation **15** disrupted cellular DNA, resulting in an elevated amount of DNA in the comet tails.

Cell cycle arrest enabling DNA repair or induction of apoptosis is often promoted by p53 activation. The slightly increased levels of p53 before its complete vanishing observed in ARN8 cells (Figs. 5B and 6C) led us to utilize A375-derived ARN8 cells stably transfected with a p53-responsive reporter construct. This approach enabled the analysis of p53 transcriptional activity by measuring β-galactosidase activity. The results clearly showed an escalation in transcriptional activity of p53 after treatment with **15** and exposure to blue light (Fig. 8). The drop of the activity at the higher tested concentrations of **15** correlates with the disappearance of the protein observed in immunoblotting analysis

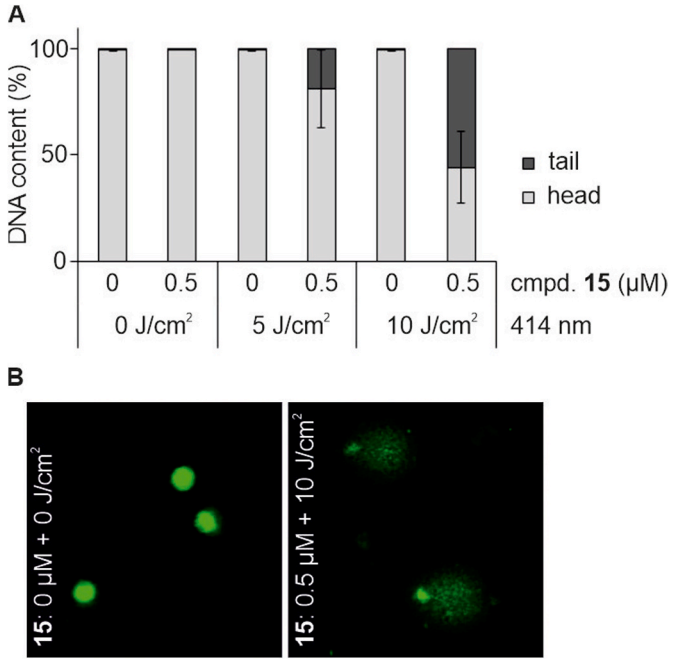


**Fig. 7.** DNA damage detected by a comet assay in G361 cells. (**A**) Percentual DNA content in the comet heads (nuclei) and tails of G361 cells treated with **15** (0.5 μM) and irradiated with indicated doses of blue light (414 nm). (**B**) Representative figures of DNA damage in G361 cells visualized by SYBR Green.

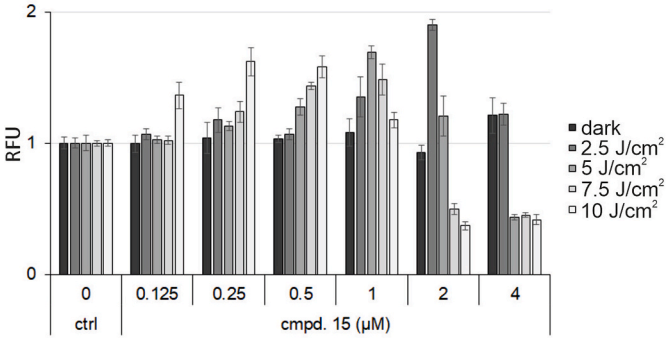


**Fig. 8.** Effect of **15** on p53-dependent transcription in ARN8 cells stably transfected with a p53-responsive β-galactosidase reporter construct. ARN8 cells were treated with increasing concentrations of **15** for 4 h, irradiated with indicated energy doses of blue light (414 nm) and incubated for further 20 h.

(Fig. 6C). Although the role of p53 in the response of cancer cells to photodynamic therapy has not been clearly elucidated [57], a higher sensitivity of p53-positive cells to PTD has been reported, for example in a study with 5-aminolevulinic acid [56].

## 3. Conclusions

This study describes an efficient synthesis of 2-phenylethenyl-1*H*-benzo[*e*]indoles through a Knoevenagel-type reaction using commercially available 1,1,2-trimethyl-1*H*-benzo[*e*]indole **1** and variously substituted benzaldehydes. Most synthesized compounds exhibited photocytotoxicity upon irradiation with blue light, with efficacy highly dependent on the substitution pattern of the compound. Structure-activity relationship analysis revealed that compounds with electron-withdrawing groups, such as nitro and cyano substituents, generally demonstrated higher photo-induced cytotoxicity, whereas those with electron-donating groups were less effective.

Compound **15**, in particular, showed notable effectiveness, exhibiting a significant increase in cytotoxicity under blue light exposure compared to dark conditions. Furthermore, the cytotoxicity of compound **15** was found to be light energy-dependent, with higher irradiation doses resulting in more pronounced effects. The strong photo-induced activity of compound **15** was linked to increased ROS generation and subsequent induction of apoptosis, as evidenced by changes in specific protein markers.

Overall, these findings enhance our understanding of the compounds' photocytotoxic properties, lay a foundation for further optimization of this type of photosensitizers for cancer treatment, underscore therapeutic potential of blue light, and suggest potential pathways for improving photodynamic therapy.

## 4. Experimental

### 4.1. Chemistry

#### 4.1.1. General

All chemicals and solvents were purchased from commercial suppliers and used without further purification unless otherwise specified. The $^{1}$H, $^{13}$C NMR spectra were recorded in $CDCl_3$ solutions at 25 °C on a Bruker Avance III 700 (700 MHz for $^{1}$H, 176 MHz for $^{13}$C, 71 MHz for $^{15}$N) spectrometer equipped with a 5 mm TCI $^{1}$H–$^{13}$C/$^{15}$N/D z-gradient cryoprobe (Bruker BioSpin GmbH, Rheinstetten, Germany). The chemical shifts, expressed in ppm, were relative to tetramethylsilane (TMS). The $^{15}$N NMR spectra were referenced to neat, external nitromethane. The $^{19}$F NMR spectra (376 MHz, absolute referencing *via* Ξ ratio) were recorded on a Bruker Avance III 400 spectrometer (Bruker BioSpin AG, Fällanden, Switzerland) with a 'directly' detecting broadband observe probe (BBO). The chemical shifts ($\delta$), expressed in ppm, were relative to tetramethylsilane (TMS). FT-IR spectra were collected using the ATR method on a Bruker Vertex 70v spectrometer (Bruker Optik GmbH, Ettlingen, Germany) with an integrated Platinum ATR accessory. The melting points of crystalline compounds were determined in open capillary tubes (temperature gradient – 2 °C/min) with a Buchi M − 565 apparatus (Büchi Labortechnik AG, Flawil, Switzerland) and are uncorrected. High-resolution mass spectrometry (HRMS) spectra were obtained in ESI mode with a Bruker MicrOTOF-Q III spectrometer (Bruker Daltonik GmbH, Bremen, Germany). Reactions were performed in Teflon cap sealed 10 mL glass vials with magnetic stirring. Reaction progress was monitored by TLC analysis on Macherey-Nagel™ ALUGRAM® Xtra SIL G/UV$_{254}$ plates (Macherey-Nagel GmbH & Co., Düren, Germany). TLC plates were visualized with UV light (wavelengths 254 and 365 nm). Compounds were purified by flash chromatography in a glass column (stationary phase – silica gel 60, 0.063–0.200 mm, 70–230 mesh ASTM, supplier Merck KGaA, Darmstadt, Germany). The UV–Vis spectra were recorded on a Shimadzu 2600 UV/Vis spectrophotometer (Shimadzu Corporation, Japan). The fluorescence spectra were recorded on an FLS920 fluorescence spectrometer from Edinburgh Instruments (Edinburgh Analytical Instruments Limited, Edinburgh, UK). All the optical measurements were performed at room temperature under ambient conditions.

#### 4.1.2. General procedure for the synthesis of compounds 2-21

1,1,2-Trimethyl-1*H*-benzo[*e*]indole **1** (1 mmol, 1 eq.) was dissolved in ethanol (2 mL) and appropriate benzaldehyde (1–1.5 mmol, 1–1.5 eq.), piperidine (90 μL) and acetic acid (100 μL) were added. The reaction mixture was stirred at reflux for 24 h. Upon cooling, the solvent was removed under reduced pressure and the residue was subjected to column chromatography on silica gel or the resulting crystals were filtered, washed with ethanol, and dried.

*4.1.2.1. 1,1-Dimethyl-2-[(E)-2-phenylethenyl]-1H-benzo[e]indole **(2)**.* Compound **2** was synthesized according to the General procedure using benzaldehyde (0.15 mL, 1.5 mmol). After flash chromatography on silica gel (eluent – *n*-hexane/ethyl acetate 9/1 *v/v*), **2** was obtained as a yellow solid (233 mg, 83 % yield). M.p. 104–105 °C. $R_f$ = 0.38 (*n*-hexane/ethyl acetate 6/1 *v/v*). $^{1}$H NMR (700 MHz, $CDCl_3$): $\delta$ 8.06 (d, $J$ = 8.3 Hz, 1H, 9-H), 7.95 (d, $J$ = 6.9 Hz, 1H, 6-H), 7.90–7.83 (m, 3H, 4,5-H, –CH=C<u>H</u>-Ph), 7.65 (d, $J$ = 7.4 Hz, 2H, Ph 2,6-H), 7.56 (ddd, $J$ = 8.2, 6.7, 1.3 Hz, 1H, 8-H), 7.45 (ddd, $J$ = 8.1, 6.8, 1.1 Hz, 1H, 7-H), 7.41 (t, $J$ = 7.6 Hz, 2H, Ph 3,5-H), 7.38–7.33 (m, 1H, Ph 4-H), 7.15 (d, $J$ = 16.2 Hz, 1H, -C<u>H</u>=CH-Ph), 1.69 (s, 6H, 1-$(CH_3)_2$). $^{13}$C NMR (176 MHz, $CDCl_3$): $\delta$ 185.0 (C-2), 151.2 (C-3a), 139.5 (C-9b), 137.6 (-CH=<u>C</u>H-Ph), 136.1 (Ph C-1), 132.6 (C-5a), 129.7 (C-6a), 129.3 (Ph C-4), 129.2 (C-5), 128.9 (Ph C-3,5), 128.5 (C-9a), 127.5 (Ph C-2,6), 126.4 (C-8), 124.6 (C-7), 122.8 (C-9), 120.4 (C-4), 119.1 (-<u>C</u>H=CH-Ph), 54.4 (C-1), 23.1 (1-$(CH_3)_2$). $^{15}$N NMR (71 MHz, $CDCl_3$): $\delta$ −74.8 (N-3). IR (ATR): $\nu$ = 3056 (m), 3038 (w), 3023 (w), 2977 (m), 2968 (m), 2931 (m), 2868 (w) cm$^{-1}$ ($CH_{arom}$, $CH_{aliph}$). HRMS (ESI-TOF) *m/z* $[M+H]^+$ calcd. for $C_{22}H_{20}N$: 298.1590, found: 298.1592.

*4.1.2.2. 2-[(E)-2-(4-Methoxyphenyl)ethenyl]-1,1-dimethyl-1H-benzo[e]indole **(3)**.* Compound **3** was synthesized according to the General procedure using 4-methoxybenzaldehyde (0.18 mL, 1.5 mmol). After flash chromatography on silica gel (eluent – *n*-hexane/ethyl acetate 6/1 *v/v*), **3** was obtained as a yellow-orange solid (168 mg, 52 % yield). M.p. 135–137 °C. $R_f$ = 0.19 (*n*-hexane/ethyl acetate 6/1 *v/v*). $^{1}$H NMR (700 MHz, $CDCl_3$): $\delta$ 8.04 (d, $J$ = 8.4 Hz, 1H, 9-H), 7.94 (d, $J$ = 8.2 Hz, 1H, 6-H), 7.89–7.80 (m, 3H, 4,5-H, –CH=C<u>H</u>-Ph), 7.59 (d, $J$ = 8.7 Hz, 2H, Ph 2,6-H), 7.57–7.52 (m, 1H, 8-H), 7.46–7.41 (m, 1H, 7-H), 7.01 (d, $J$ = 16.2 Hz, 1H, -C<u>H</u>=CH-Ph), 6.93 (d, $J$ = 8.7 Hz, 2H, Ph 3,5-H), 3.83 (s, 3H, –$OCH_3$), 1.68 (s, 6H, 1-$(CH_3)_2$). $^{13}$C NMR (176 MHz, $CDCl_3$): $\delta$ 185.4 (C-2), 160.7 (Ph C-4), 151.3 (C-3a), 139.3 (C-9b), 137.3 (-CH=<u>C</u>H-Ph), 132.4 (C-5a), 129.7 (C-6), 129.1 (Ph C-2,6), 129.0 (C-5), 128.9 (Ph C-1), 128.5 (C-9a), 126.3 (C-8), 124.4 (C-7), 122.7 (C-9), 120.3 (C-4), 116.8 (-<u>C</u>H=CH-Ph), 114.4 (Ph C-3,5), 55.4 (-$OCH_3$), 54.3 (C-1), 23.2 (1-$(CH_3)_2$). $^{15}$N NMR (71 MHz, $CDCl_3$): $\delta$ −78.4 (N-3). IR (ATR): $\nu$ = 3043 (m), 3001 (w), 2973 (m), 2960 (m), 2931 (m), 2867 (w), 2833 (w) cm$^{-1}$ ($CH_{arom}$, $CH_{aliph}$). HRMS (ESI-TOF) *m/z* $[M+H]^+$ calcd. for $C_{23}H_{22}NO$: 328.1696, found: 328.1698.

*4.1.2.3. 4-[(E)-2-(1,1-Dimethyl-1H-benzo[e]indol-2-yl)ethenyl]-N,N-dimethylaniline **(4)**, previously reported in Ref. [25].* Compound **4** was synthesized using 4-(dimethylamino)benzaldehyde (212 mg, 1.5 mmol). After flash chromatography on silica gel (eluent – *n*-hexane/ethyl acetate 6/1 v/v), **4** was obtained as a reddish-brown amorphous material (68 mg, 21 % yield). $R_f$ = 0.13 (*n*-hexane/ethyl acetate 6/1 *v/v*). $^{1}$H NMR (700 MHz, $CDCl_3$): $\delta$ 8.05 (d, $J$ = 9.4 Hz, 1H, 9-H), 7.93 (d, $J$ = 9.5 Hz, 1H, 6-H), 7.87–7.79 (m, 3H, 4,5-H, –CH=C<u>H</u>-Ph), 7.54 (t, $J$ = 8.3 Hz, 3H, Ph 3,5-H, 8-H), 7.45–7.40 (m, 1H, 7-H), 6.93 (d, $J$ = 16.1 Hz, 1H, -C<u>H</u>=CH-Ph), 6.72 (d, $J$ = 8.8 Hz, 2H, Ph 2,6-H), 3.02 (s, 6H, –N$(CH_3)_2$), 1.68 (s, 6H, 1-$(CH_3)_2$). $^{13}$C NMR (176 MHz, $CDCl_3$): $\delta$ 185.9

(C-2), 151.6 (C-3a), 151.2 (Ph C-1), 139.1 (C-9b), 138.2 (-CH=CH-Ph), 132.3 (C-5a), 129.7 (C-6), 129.1 (Ph C-3,5), 129.0 (C-5), 128.6 (C-9a), 126.2 (C-8), 124.2 (C-7), 124.1 (Ph C-4), 122.7 (C-9), 120.2 (C-4), 114.1 (-CH=CH-Ph), 112.1 (Ph C-2,6), 54.2 (C-1), 40.2 (-N($CH_3$)$_2$), 23.5 (1-($CH_3$)$_2$). $^{15}$N NMR (71 MHz, $CDCl_3$): $\delta$ −83.4 (N-3), −330.0 (N($CH_3$)$_2$). HRMS (ESI-TOF) *m/z* $[M+H]^+$ calcd. for $C_{24}H_{25}N_2$: 341.2012, found: 341.2010.

*4.1.2.4. 4-[(E)-2-(1,1-Dimethyl-1H-benzo[e]indol-2-yl)ethenyl]-N,N-diethylaniline (**5**).* Compound **5** was synthesized using 4-(diethylamino) benzaldehyde (254 mg, 1.5 mmol). After flash chromatography on silica gel (eluent – *n*-hexane/ethyl acetate 4/1 *v/v*), **5** was obtained as a brown amorphous material (55 mg, 16 % yield). $R_f$ = 0.26 (*n*-hexane/ethyl acetate 6/1 *v/v*). $^1$H NMR (700 MHz, $CDCl_3$): $\delta$ 8.05 (d, $J$ = 8.2 Hz, 1H, 9-H), 7.93 (d, $J$ = 8.1 Hz, 1H, 6-H), 7.87–7.81 (m, 2H, 4,5-H), 7.80 (d, $J$ = 16.1 Hz, 1H, –CH=CH-Ph), 7.56–7.50 (m, 3H, 8-H, Ph 3,5-H), 7.45–7.40 (m, 1H, 7-H), 6.90 (d, $J$ = 16.0 Hz, 1H, -CH=CH-Ph), 6.68 (d, $J$ = 8.8 Hz, 2H, Ph 2,6-H), 3.41 (q, $J$ = 7.1 Hz, 4H, –N($CH_2CH_3$)$_2$), 1.68 (s, 6H, 1-($CH_3$)$_2$), 1.20 (t, $J$ = 7.1 Hz, 6H, –N($CH_2CH_3$)$_2$). $^{13}$C NMR (176 MHz, $CDCl_3$): $\delta$ 186.1 (C-2), 151.6 (C-3a), 148.7 (Ph C-1), 139.1 (C-9b), 138.3 (-CH=CH-Ph), 132.2 (C-5a), 129.7 (C-6), 129.4 (Ph C-3,5), 129.0 (C-5), 128.6 (C-9a), 126.2 (C-8), 124.1 (C-7), 123.2 (Ph C-4), 122.7 (C-9), 120.2 (C-4), 113.5 (-CH=CH-Ph), 111.5 (Ph C-2,6), 54.2 (C-1), 44.5 (-N($CH_2CH_3$)$_2$), 23.5 (1-($CH_3$)$_2$), 12.6 (-N($CH_2CH_3$)$_2$). $^{15}$N NMR (71 MHz, $CDCl_3$): $\delta$ −84.6 (N-3), −300.4 (N($CH_2CH_3$)$_2$). IR (ATR): $\nu$ = 3030 (w), 2970 (s), 2928 (m), 2889 (w), 2869 (w) cm$^{-1}$ ($CH_{arom}$, $CH_{aliph}$). HRMS (ESI-TOF) *m/z* $[M+H]^+$ calcd. for $C_{26}H_{29}N_2$: 369.2325, found: 369.2322.

*4.1.2.5. 2-[(E)-2-(4-Bromophenyl)ethenyl]-1,1-dimethyl-1H-benzo[e]indole (**6**).* Compound **6** was synthesized according to the General procedure using 4-bromobenzaldehyde (278 mg, 1.5 mmol). After flash chromatography on silica gel (eluent – *n*-hexane/ethyl acetate 6/1 *v/v*), **6** was obtained as a yellow-orange solid (294 mg, 77 % yield). M.p. 140–141 °C. $R_f$ = 0.41 (*n*-hexane/ethyl acetate 6/1 *v/v*). $^1$H NMR (700 MHz, $CDCl_3$): $\delta$ 8.05 (d, $J$ = 8.4 Hz, 1H, 9-H), 7.96 (d, $J$ = 8.7 Hz, 1H, 6-H), 7.91–7.83 (m, 2H, 4,5-H), 7.78 (d, $J$ = 16.2 Hz, 1H, –CH=CH-Ph), 7.59–7.44 (m, 6H, Ph 2,3,5,6-H, 7,8-H), 7.12 (d, $J$ = 16.2 Hz, 1H, -CH=CH-Ph), 1.68 (s, 6H, 1-($CH_3$)$_2$). $^{13}$C NMR (176 MHz, $CDCl_3$): $\delta$ 184.7 (C-2), 151.1 (C-3a), 139.5 (C-9b), 136.2 (-CH=CH-Ph), 135.0 (Ph C-1), 132.6 (C-5a), 132.1 (Ph C-3,5), 129.7 (C-6), 129.2 (C-5), 128.9 (Ph C-2,6), 128.5 (C-9a), 126.4 (C-8), 124.7 (C-7), 123.3 (Ph C-4), 122.8 (C-9), 120.4 (C-4), 119.6 (-CH=CH-Ph), 54.4 (C-1), 23.0 (1-($CH_3$)$_2$). $^{15}$N NMR (71 MHz, $CDCl_3$): $\delta$ −73.6 (N-3). IR (ATR): $\nu$ = 3049 (w), 2968 (s), 2927 (m), 2866 (w) cm$^{-1}$ ($CH_{arom}$, $CH_{aliph}$). HRMS (ESI-TOF) *m/z* $[M+H]^+$ calcd. for $C_{22}H_{19}BrN$: 376.0695, found: 376.0693.

*4.1.2.6. 1,1-Dimethyl-2-[(E)-2-(4-nitrophenyl)ethenyl]-1H-benzo[e]indole (**7**).* Compound **7** was synthesized according to the General procedure using 4-nitrobenzaldehyde (227 mg, 1.07 mmol). Yellow-orange solid (267 mg, 76 % yield). M.p. 215–216 °C. $R_f$ = 0.26 (*n*-hexane/ethyl acetate 6/1 *v/v*). $^1$H NMR (700 MHz, $CDCl_3$): $\delta$ 8.29–8.25 (m, 2H, Ph 3,5-H), 8.07 (d, $J$ = 8.4 Hz, 1H, 9-H), 7.97 (d, $J$ = 7.1 Hz, 1H, 6-H), 7.92–7.86 (m, 3H, 4,5-H, –CH=CH-Ph), 7.77 (d, $J$ = 8.7 Hz, 2H, Ph 2,6-H), 7.61–7.56 (m, 1H, 8-H), 7.52–7.47 (m, 1H, 7-H), 7.27 (d, $J$ = 16.2 Hz, 1H, -CH=CH-Ph), 1.71 (s, 6H, 1-($CH_3$)$_2$). $^{13}$C NMR (176 MHz, $CDCl_3$): $\delta$ 184.0 (C-2), 151.0 (C-3a), 147.7 (Ph C-4), 142.4 (Ph C-1), 139.8 (C-9b), 134.6 (-CH=CH-Ph), 132.9 (C-5a), 129.8 (C-6), 129.4 (C-5), 128.4 (C-9a), 128.0 (Ph C-2,6), 126.6 (C-8), 125.0 (C-7), 124.3 (Ph C-3,5), 123.1 (-CH=CH-Ph), 122.9 (C-9), 120.5 (C-4), 54.5 (C-1), 22.9 (1-($CH_3$)$_2$). $^{15}$N NMR (71 MHz, $CDCl_3$): $\delta$ −67.8 (N-3), −13.1 (-$NO_2$). IR (ATR): $\nu$ = 1509 (vs), 1342 (s) cm$^{-1}$ (-$NO_2$). HRMS (ESI-TOF) *m/z* $[M+H]^+$ calcd. for $C_{22}H_{19}N_2O_2$: 343.1441, found: 343.1440.

*4.1.2.7. 1,1-Dimethyl-2-[(E)-2-(3-nitrophenyl)ethenyl]-1H-benzo[e]indole (**8**).* Compound **8** was synthesized according to the General procedure using 3-nitrobenzaldehyde (180 mg, 1.2 mmol). Yellow solid (280 mg, 82 % yield). M.p. 176–177 °C. $R_f$ = 0.11 (*n*-hexane/ethyl acetate 6/1 *v/v*). $^1$H NMR (700 MHz, $CDCl_3$): $\delta$ 8.51 (s, 1H, Ph 2-H), 8.20 (d, $J$ = 8.1 Hz, 1H, Ph 6-H), 8.07 (d, $J$ = 8.4 Hz, 1H, 9-H), 7.97 (d, $J$ = 8.2 Hz, 1H, 6-H), 7.93–7.85 (m, 4H, Ph 4-H, –CH=CH-Ph, 4,5-H), 7.62–7.57 (m, 2H, Ph 5-H, 8-H), 7.51–7.47 (m, 1H, 7-H), 7.25 (d, $J$ = 16.2 Hz, 1H, -CH=CH-Ph), 1.72 (s, 6H, 1-($CH_3$)$_2$). $^{13}$C NMR (176 MHz, $CDCl_3$): $\delta$ 184.1 (C-2), 151.0 (C-3a), 148.8 (Ph C-1), 139.7 (C-9b), 137.9 (Ph C-3), 134.6 (-CH=CH-Ph), 133.4 (Ph C-4), 132.8 (C-5a), 129.9 (Ph C-5), 129.8 (C-6), 129.4 (C-5), 128.5 (C-9a), 126.6 (C-8), 124.9 (C-7), 123.5 (Ph C-6), 122.9 (C-9), 121.8 (-CH=CH-Ph), 121.6 (Ph C-2), 120.5 (C-4), 54.5 (C-1), 22.9 (1-($CH_3$)$_2$). $^{15}$N NMR (71 MHz, $CDCl_3$): $\delta$ −69.8 (N-3), −12.9 (-$NO_2$). IR (ATR): $\nu$ = 1522 (vs), 1346 (s) cm$^{-1}$ (-$NO_2$). HRMS (ESI-TOF) *m/z* $[M+H]^+$ calcd. for $C_{22}H_{19}N_2O_2$: 343.1441, found: 343.1439.

*4.1.2.8. 1,1-Dimethyl-2-[(E)-2-(2-nitrophenyl)ethenyl]-1H-benzo[e]indole (**9**).* Compound **9** was synthesized according to the General procedure using 2-nitrobenzaldehyde (181 mg, 1.2 mmol). After flash chromatography on silica gel (eluent – *n*-hexane/ethyl acetate 5/3 *v/v*), **9** was obtained as yellow-orange amorphous material (174 mg, 51 % yield). $R_f$ = 0.66 (*n*-hexane/ethyl acetate 1/1 *v/v*). $^1$H NMR (700 MHz, $CDCl_3$): $\delta$ 8.16 (d, $J$ = 16.5 Hz, 1H, –CH=CH-Ph), 8.10 (d, $J$ = 8.4 Hz, 1H, 9-H), 8.07 (d, $J$ = 7.9 Hz, 1H, Ph 3-H), 7.97 (d, $J$ = 8.2 Hz, 1H, 6-H), 7.90 (d, $J$ = 8.5 Hz, 1H, 5-H), 7.87 (d, $J$ = 8.4 Hz, 1H, 4-H), 7.84 (d, $J$ = 7.2 Hz, 1H, Ph 6-H), 7.69 (t, $J$ = 7.5 Hz, 1H, Ph 5-H), 7.59 (t, $J$ = 7.4 Hz, 1H, 8-H), 7.54–7.47 (m, 2H, 7-H, Ph 4-H), 7.18 (d, $J$ = 16.5 Hz, 1H, -CH=CH-Ph), 1.77 (s, 6H, 1-($CH_3$)$_2$). $^{13}$C NMR (176 MHz, $CDCl_3$): $\delta$ 184.2 (C-2), 150.9 (C-3a), 148.2 (Ph C-1), 140.6 (C-9b), 133.5 (Ph C-5), 133.0 (C-5a), 132.4 (-CH=CH-Ph), 132.3 (Ph C-2), 129.8 (C-6), 129.33 (C-5), 129.32 (Ph C-4), 128.5 (Ph C-6), 128.3 (C-9a), 126.5 (C-8), 125.9 (-CH=CH-Ph), 125.1 (Ph C-3), 125.0 (C-7), 122.9 (C-9), 120.6 (C-4), 54.6 (C-1), 23.7 (1-($CH_3$)$_2$). $^{15}$N NMR (71 MHz, $CDCl_3$): $\delta$ −61.2 (N-3), −8.8 (-$NO_2$). IR (ATR): $\nu$ = 1514 (vs), 1336 (s) cm$^{-1}$ (-$NO_2$). HRMS (ESI-TOF) *m/z* $[M+H]^+$ calcd. for $C_{22}H_{19}N_2O_2$: 343.1441, found: 343.1442.

*4.1.2.9. 4-[(E)-2-(1,1-Dimethyl-1H-benzo[e]indol-2-yl)ethenyl]benzonitrile (**10**).* Compound **10** was synthesized according to the General procedure using 4-cyanobenzaldehyde (196 mg, 1.5 mmol). After flash chromatography on silica gel (eluent – 100 % dichloromethane to *n*-hexane/ethyl acetate 3/1 *v/v*), **10** was obtained as a yellow solid (306 mg, 95 % yield). M.p. 203–204 °C. $R_f$ = 0.21 (*n*-hexane/ethyl acetate 6/1 *v/v*). $^1$H NMR (700 MHz, $CDCl_3$): $\delta$ 8.06 (d, $J$ = 8.4 Hz, 1H, 9-H), 7.97 (d, $J$ = 8.2 Hz, 1H, 6-H), 7.90 (d, $J$ = 8.5 Hz, 1H, 5-H), 7.87 (d, $J$ = 8.5 Hz, 1H, 4-H), 7.83 (d, $J$ = 16.2 Hz, 1H, –CH=CH-Ph), 7.72 (d, $J$ = 8.4 Hz, 2H), Ph 3,5-H), 7.69 (d, $J$ = 8.4 Hz, 2H, Ph 2,6-H), 7.58 (ddd, $J$ = 8.3, 6.7, 1.3 Hz, 1H, 8-H), 7.49 (ddd, $J$ = 8.0, 6.8, 1.1 Hz, 1H, 7-H), 7.22 (d, $J$ = 16.3 Hz, 1H, -CH=CH-Ph), 1.69 (s, 6H, 1-($CH_3$)$_2$). $^{13}$C NMR (176 MHz, $CDCl_3$): $\delta$ 184.1 (C-2), 151.0 (C-3a), 140.5 (Ph C-4), 139.8 (C-9b), 135.1 (-CH=CH-Ph), 132.8 (C-5a), 132.6 (Ph C-2,6), 129.8 (C-6), 129.4 (C-5), 128.4 (C-9a), 127.8 (Ph C-3,5), 126.6 (C-8), 125.0 (C-7), 122.9 (C-9), 122.4 (-CH=CH-Ph), 120.5 (C-4), 118.7 (-CN), 112.2 (Ph C-1), 54.5 (C-1), 22.9 (1-($CH_3$)$_2$). $^{15}$N NMR (71 MHz, $CDCl_3$): $\delta$ −68.9 (N-3), –CN not found. IR (ATR): $\nu$ = 2225 (vs) cm$^{-1}$ (-CN). HRMS (ESI-TOF) *m/z* $[M+H]^+$ calcd. for $C_{23}H_{19}N_2$: 323.1543, found: 323.1540.

*4.1.2.10. 3-[(E)-2-(1,1-Dimethyl-1H-benzo[e]indol-2-yl)ethenyl]benzonitrile (**11**), previously reported in Ref. [58].* Compound **11** was synthesized according to the General procedure using 3-formylbenzonitrile (156 mg, 1.2 mmol). After flash chromatography on silica gel (eluent – *n*-hexane/ethyl acetate 5/3 *v/v*), **11** was obtained as a yellow-orange solid (209 mg, 65 %). M.p. 129–130 °C. $R_f$ = 0.11 (*n*-hexane/ethyl acetate 6/1 *v/v*). $^1$H NMR (700 MHz, $CDCl_3$): $\delta$ 8.06 (d, $J$ = 8.4 Hz, 1H,

9-H), 7.97 (d, $J = 8.1$ Hz, 1H, 6-H), 7.93–7.79 (m, 5H, 4,5-H, Ph 2,4-H, –CH=CH-Ph), 7.63 (d, $J = 7.7$ Hz, 1H, Ph 6-H), 7.61–7.56 (m, 1H, 8-H), 7.53 (t, $J = 7.7$ Hz, 1H, Ph 5-H), 7.51–7.46 (m, 1H, 7-H), 7.17 (d, $J = 16.2$ Hz, 1H, -CH=CH-Ph), 1.70 (s, 6H, 1-$(CH_3)_2$). $^{13}$C NMR (176 MHz, $CDCl_3$): $\delta$ 184.1 (C-2), 151.0 (C-3a), 139.7 (C-9b), 137.4 (Ph C-3), 134.7 (-CH=CH-Ph), 132.8 (C-5a), 132.1 (Ph C-6), 131.5 (Ph C-4), 130.7 (C-5), 129.79 (Ph C-5), 129.76 (C-6), 129.4 (C-5), 128.5 (C-9a), 126.5 (C-8), 124.9 (C-7), 122.9 (C-9), 121.4 (-CH=CH-Ph), 120.4 (C-4), 118.5 (-CN), 113.3 (Ph C-1), 54.5 (C-1), 22.9 (1-$(CH_3)_2$). $^{15}$N NMR (71 MHz, $CDCl_3$): $\delta$ −70.8 (N-3), –CN not found. IR (ATR): $\nu = 2225$ (vs) cm$^{-1}$ (-CN). HRMS (ESI-TOF) $m/z$ $[M+H]^+$ calcd. for $C_{23}H_{19}N_2$: 323.1543, found: 323.1541.

*4.1.2.11. 1,1-Dimethyl-2-{(E)-2-[4-(trifluoromethyl)phenyl]ethenyl}-1H-benzo[e]indole (12).* Compound **12** was synthesized according to the General procedure using 4-(trifluoromethyl)benzaldehyde (0.16 mL, 1.2 mmol). Yellow solid (92 mg, 25 % yield). M.p. 156–157 °C. $R_f = 0.37$ (*n*-hexane/ethyl acetate 6/1 *v/v*). $^1$H NMR (700 MHz, $CDCl_3$): $\delta$ 8.07 (d, $J = 8.4$ Hz, 1H, 9-H), 7.97 (d, $J = 8.2$ Hz, 1H, 6-H), 7.92–7.84 (m, 3H, 4,5-H, –CH=CH-Ph), 7.74 (d, $J = 8.0$ Hz, 2H, Ph 2,6-H), 7.67 (d, $J = 8.0$ Hz, 2H, Ph 3,5-H), 7.61–7.56 (m, 1H, 8-H), 7.48 (t, $J = 7.5$ Hz, 1H, 7-H), 7.21 (d, $J = 16.2$ Hz, 1H, -CH=CH-Ph), 1.70 (s, 6H, 1-$(CH_3)_2$). $^{13}$C NMR (176 MHz, $CDCl_3$): $\delta$ 184.4 (C-2), 151.1 (C-3a), 139.7 (C-9b), 139.5 (Ph C-1), 135.7 (-CH=CH-Ph), 132.8 (C-5a), 130.7 (q, $^2J_{CF} = 32.5$ Hz, Ph C-4), 129.8 (C-6), 129.3 (C-5), 128.5 (C-9a), 127.6 (Ph C-2,6), 126.5 (C-8), 125.9 (q, $^3J_{CF} = 3.8$ Hz, Ph C-3,5), 124.8 (C-7), 124.0 (q, $^1J_{CF} = 272.0$ Hz, -$CF_3$), 122.8 (C-9), 121.4 (-CH=CH-Ph), 120.5 (C-4), 54.5 (C-1), 23.0 (1-$(CH_3)_2$). $^{19}$F NMR (376 MHz, $CDCl_3$): $\delta$ −62.7 ($CF_3$). $^{15}$N NMR (71 MHz, $CDCl_3$): $\delta$ −70.6 (N-3). IR (ATR): $\nu = 3047$ (m), 2978 (m), 2934 (m), 2869 (w) cm$^{-1}$ ($CH_{arom}$, $CH_{aliph}$). HRMS (ESI-TOF) $m/z$ $[M+H]^+$ calcd. for $C_{23}H_{19}F_3N$: 366.1464, found: 366.1467.

*4.1.2.12. 1,1-Dimethyl-2-{(E)-2-[3-(trifluoromethyl)phenyl]ethenyl}-1H-benzo[e]indole (13).* Compound **13** was synthesized according to the General procedure using 3-(trifluoromethyl)benzaldehyde (0.2 mL, 1.5 mmol). After flash chromatography on silica gel (eluent – *n*-hexane/ethyl acetate 6/1 *v/v*), **13** was obtained as a yellow amorphous material (310 mg, 85 % yield). $R_f = 0.36$ (*n*-hexane/ethyl acetate 6/1 *v/v*). $^1$H NMR (700 MHz, $CDCl_3$): $\delta$ 8.07 (d, $J = 8.0$ Hz, 1H, 9-H), 7.96 (d, $J = 8.2$ Hz, 1H, 6-H), 7.92–7.84 (m, 4H, 4,5-H, Ph 2-H, –CH=CH-Ph), 7.79 (d, $J = 7.7$ Hz, 1H, Ph 6-H), 7.62–7.51 (m, 3H, Ph 4,5-H, 8-H), 7.50–7.45 (m, 1H, 7-H), 7.19 (d, $J = 16.2$ Hz, 1H, -CH=CH-Ph), 1.71 (s, 6H, 1-$(CH_3)_2$). $^{13}$C NMR (176 MHz, $CDCl_3$): $\delta$ 184.4 (C-2), 151.1 (C-3a), 139.7 (C-9b), 136.9 (Ph C-1), 135.7 (-CH=CH-Ph), 132.7 (C-5a), 131.4 (q, $^2J_{CF} = 32.3$ Hz, Ph C-3), 130.7 (Ph C-6), 129.7 (C-6), 129.4 (q, $^3J_{CF} = 3.8$ Hz, Ph C-2), 129.3 (C-5), 128.5 (C-9a), 126.5 (C-8), 125.6 (q, $^3J_{CF} = 3.7$ Hz, Ph C-4), 124.8 (C-7), 124.0 (q, $^1J_{CF} = 272.4$ Hz, -$CF_3$), 123.9 (q, $^3J_{CF} = 3.8$ Hz, Ph C-2), 122.9 (C-9), 120.9 (-CH=CH-Ph), 120.4 (C-4), 54.5 (C-1), 23.0 (1-$(CH_3)_2$). $^{19}$F NMR (376 MHz, $CDCl_3$): $\delta$ −62.8 ($CF_3$). $^{15}$N NMR (71 MHz, $CDCl_3$): $\delta$ −71.4 (N-3). IR (ATR): $\nu = 3059$ (w), 2975 (m), 2932 (m), 2870 (w) cm$^{-1}$ ($CH_{arom}$, $CH_{aliph}$). HRMS (ESI-TOF) $m/z$ $[M+H]^+$ calcd. for $C_{23}H_{19}F_3N$: 366.1464, found: 366.1466.

*4.1.2.13. 2-[(E)-2-(4-Fluorophenyl)ethenyl]-1,1-dimethyl-1H-benzo[e]indole (14).* Compound **14** was synthesized according to the General procedure I using 4-fluorobenzaldehyde (0.15 mL, 1.5 mmol). After flash chromatography on silica gel (eluent – *n*-hexane/ethyl acetate 6/1 *v/v*), **14** was obtained as a yellow amorphous material (216 mg, 69 % yield). $R_f = 0.46$ (*n*-hexane/ethyl acetate 4/1 *v/v*). $^1$H NMR (700 MHz, $CDCl_3$): $\delta$ 8.05 (d, $J = 8.4$ Hz, 1H, 9-H), 7.95 (d, $J = 8.3$ Hz, 1H, 6-H), 7.89–7.84 (m, 2H, 4,5-H), 7.82 (d, $J = 16.2$ Hz, 1H, –CH=CH-Ph), 7.63–7.59 (m, 2H, Ph 2,6-H), 7.58–7.53 (m, 1H, 8-H), 7.47–7.42 (m, 1H, 7-H), 7.12–7.07 (m, 2H, Ph 3,5-H), 7.05 (d, $J = 16.2$ Hz, 1H, -CH=CH-Ph), 1.68 (s, 6H, 1-$(CH_3)_2$). $^{13}$C NMR (176 MHz, $CDCl_3$): $\delta$ 184.9 (C-2), 163.3 (d, $^1J_{CF} = 249.9$ Hz, Ph C-4), 151.2 (C-3a), 139.4 (C-9b), 136.3 (-CH=CH-Ph), 132.6 (C-5a), 132.4 (d, $^4J_{CF} = 3.3$ Hz, Ph C-1), 129.7 (C-6), 129.21 (d, $^3J_{CF} = 7.9$ Hz, Ph C-2,6), 129.19 (C-5), 128.5 (C-9a), 126.4 (C-8), 124.6 (C-7), 122.8 (C-9), 120.4 (C-4), 118.76 (d, $^6J_{CF} = 2.4$ Hz, -CH=CH-Ph), 116.0 (d, $^2J_{CF} = 21.7$ Hz, Ph C-3,5), 54.4 (C-1), 23.1 (1-$(CH_3)_2$). $^{19}$F NMR (376 MHz, $CDCl_3$): $\delta$ −111.1). $^{15}$N NMR (71 MHz, $CDCl_3$): $\delta$ −74.8 (N-3). IR (ATR): $\nu = 3068$ (w), 3047 (w), 2971 (m), 2930 (w), 2868 (w) cm$^{-1}$ ($CH_{arom}$, $CH_{aliph}$). HRMS (ESI-TOF) $m/z$ $[M+H]^+$ calcd. for $C_{22}H_{19}FN$: 316.1496, found: 316.1499.

*4.1.2.14. 2-[(E)-2-(4-Methoxy-3-nitrophenyl)ethenyl]-1,1-dimethyl-1H-benzo[e]indole (15).* Compound **15** was synthesized according to the General procedure using 4-methoxy-3-nitrobenzaldehyde (216 mg, 1.2 mmol). Orange solid (287 mg, 77 % yield). M.p. 197–198 °C. $R_f = 0.33$ (*n*-hexane/ethyl acetate 1/1 *v/v*). $^1$H NMR (700 MHz, $CDCl_3$): $\delta$ 8.16 (d, $J = 2.3$ Hz, 1H, Ph 2-H), 8.06 (d, $J = 8.4$ Hz, 1H, 9-H), 7.96 (d, $J = 8.2$ Hz, 1H, 6-H), 7.89 (d, $J = 8.5$ Hz, 1H, 5-H), 7.85 (d, $J = 8.5$ Hz, 1H, 4-H), 7.79 (d, $J = 16.2$ Hz, 1H, –CH=CH-Ph), 7.78–7.76 (m, 1H, Ph 6-H), 7.58 (t, $J = 7.5$ Hz, 1H, 8-H), 7.47 (t, $J = 7.5$ Hz, 1H, 7-H), 7.14 (d, $J = 8.7$ Hz, 1H, Ph 5-H), 7.07 (d, $J = 16.2$ Hz, 1H, -CH=CH-Ph), 4.02 (s, 3H, –$OCH_3$), 1.69 (s, 6H, 1-$(CH_3)_2$). $^{13}$C NMR (176 MHz, $CDCl_3$): $\delta$ 184.4 (C-2), 153.3 (Ph C-4), 151.1 (C-3a), 140.0 (Ph C-3), 139.6 (C-9b), 134.4 (-CH=CH-Ph), 133.3 (Ph C-6), 132.7 (C-5a), 129.7 (C-6), 129.3 (C-5), 129.0 (Ph C-1), 128.5 (C-9a), 126.5 (C-8), 124.8 (C-7), 124.0 (Ph C-2), 122.8 (C-9), 120.4 (C-4), 119.6 (-CH=CH-Ph), 113.9 (Ph C-5), 56.8 (-$OCH_3$), 54.4 (C-1), 23.0 (1-$(CH_3)_2$). $^{15}$N NMR (71 MHz, $CDCl_3$): $\delta$ −73.2 (N-3), −12.7 (-$NO_2$). IR (ATR): $\nu = 1528$ (vs), 1348 (vs) cm$^{-1}$ (-$NO_2$). HRMS (ESI-TOF) $m/z$ $[M+H]^+$ calcd. for $C_{23}H_{21}N_2O_3$: 373.1547, found: 373.1550.

*4.1.2.15. 1,1-Dimethyl-2-[(E)-2-(4-methyl-3-nitrophenyl)ethenyl]-1H-benzo[e]indole (16).* Compound **16** was synthesized according to the General procedure using 4-methyl-3-nitrobenzaldehyde (247 mg, 1.5 mmol). Yellow solid (295 mg, 83 % yield). M.p. 185–186 °C. $R_f = 0.19$ (*n*-hexane/ethyl acetate 6/1 *v/v*). $^1$H NMR (700 MHz, $CDCl_3$): $\delta$ 8.25 (d, $J = 1.9$ Hz, 1H, Ph 2-H), 8.07 (d, $J = 8.4$ Hz, 1H, 9-H), 7.96 (d, $J = 8.2$ Hz, 1H, 6-H), 7.90 (d, $J = 8.5$ Hz, 1H, 5-H), 7.86 (d, $J = 8.5$ Hz, 1H, 4-H), 7.83 (d, $J = 16.2$ Hz, 1H, –CH=CH-Ph), 7.73 (dd, $J = 7.9$, 1.9 Hz, 1H, Ph 6-H), 7.60–7.56 (m, 1H, 8-H), 7.50–7.45 (m, 1H, 7-H), 7.39 (d, $J = 7.9$ Hz, 1H, Ph 5-H), 7.18 (d, $J = 16.2$ Hz, 1H, -CH=CH-Ph), 2.64 (s, 3H, Ph –$CH_3$), 1.70 (s, 6H, 1-$(CH_3)_2$). $^{13}$C NMR (176 MHz, $CDCl_3$): $\delta$ 184.3 (C-2), 151.0 (C-3a), 149.6 (Ph C-3), 139.7 (C-9b), 135.5 (Ph C-1), 134.6 (-CH=CH-Ph), 134.2 (Ph C-4), 133.4 (Ph C-5), 132.8 (C-5a), 131.6 (Ph C-6), 129.7 (C-6), 129.3 (C-5), 128.5 (C-9a), 126.5 (C-8), 124.8 (C-7), 123.0 (Ph C-2), 122.9 (C-9), 120.9 (-CH=CH-Ph), 120.4 (C-4), 54.5 (C-1), 22.9 (1-$(CH_3)_2$), 20.5 (4-$CH_3$ Ph). $^{15}$N NMR (71 MHz, $CDCl_3$): $\delta$ −70.9 (N-3), −7.7 (-$NO_2$). IR (ATR): $\nu = 1525$ (vs), 1340 (s) cm$^{-1}$ (-$NO_2$). HRMS (ESI-TOF) $m/z$ $[M+H]^+$ calcd. for $C_{23}H_{21}N_2O_2$: 357.1598, found: 357.1595.

*4.1.2.16. 2-[(E)-2-(4-Chloro-3-nitrophenyl)ethenyl]-1,1-dimethyl-1H-benzo[e]indole (17).* Compound **17** was synthesized according to the General procedure using 4-chloro-3-nitrobenzaldehyde (222 mg, 1.2 mmol). Yellow solid (139 mg, 37 % yield). M.p. 179–180 °C. $R_f = 0.14$ (*n*-hexane/ethyl acetate 6/1 *v/v*). $^1$H NMR (700 MHz, $CDCl_3$): $\delta$ 8.13 (s, 1H, Ph 2-H), 8.06 (d, $J = 8.4$ Hz, 1H, 9-H), 7.97 (d, $J = 8.2$ Hz, 1H, 6-H), 7.91 (d, $J = 8.5$ Hz, 1H, 5-H), 7.86 (d, $J = 8.5$ Hz, 1H, 4-H), 7.80 (d, $J = 16.2$ Hz, 1H, –CH=CH-Ph), 7.73 (d, $J = 7.7$ Hz, 1H, Ph 6-H), 7.61–7.57 (m, 2H, 8-H, Ph 5-H), 7.49 (t, $J = 7.5$ Hz, 1H, 7-H), 7.18 (d, $J = 16.2$ Hz, 1H, -CH=CH-Ph), 1.69 (s, 6H, 1-$(CH_3)_2$). $^{13}$C NMR (176 MHz, $CDCl_3$): $\delta$ 183.8 (C-2), 151.0 (C-3a), 148.3 (Ph C-3), 139.8 (C-9b), 136.3 (Ph C-1), 133.4 (-CH=CH-Ph), 132.9 (C-5a), 132.4 (Ph C-5), 131.6 (Ph C-6), 129.8 (C-6), 129.4 (C-5), 128.5 (C-9a), 127.0 (Ph C-4), 126.6 (C-8), 125.0 (C-7), 123.7 (Ph C-2), 122.9 (C-9), 122.2 (-CH=CH-Ph), 120.5 (C-4), 54.5 (C-1), 22.8 (1-$(CH_3)_2$). $^{15}$N NMR (71 MHz, $CDCl_3$): $\delta$ −68.5 (N-3), −13.9 (-$NO_2$). IR (ATR): $\nu = 1527$ (vs), 1340 (s) cm$^{-1}$ (-$NO_2$). HRMS

(ESI-TOF) *m/z* $[M+H]^+$ calcd. for $C_{22}H_{18}ClN_2O_2$: 377.1051, found: 377.1049.

*4.1.2.17. 4-[(E)-2-(1,1-Dimethyl-1H-benzo[e]indol-2-yl)ethenyl]-2-fluorobenzonitrile (**18**).* Compound **18** was synthesized according to the General procedure using 4-cyano-3-fluorobenzaldehyde (148 mg, 1 mmol). After flash chromatography on silica gel (eluent – *n*-hexane/ethyl acetate 5/3 *v/v*), **18** was obtained as a yellow-orange solid (80 mg, 24 % yield). M.p. 198–199 °C. $R_f = 0.11$ (*n*-hexane/ethyl acetate 6/1 *v/v*). $^1$H NMR (700 MHz, $CDCl_3$): $\delta$ 8.06 (d, $J = 8.4$ Hz, 1H, 9-H), 7.97 (d, $J = 8.2$ Hz, 1H, 6-H), 7.91 (d, $J = 8.5$ Hz, 1H, 5-H), 7.87 (d, $J = 8.5$ Hz, 1H, 4-H), 7.79 (d, $J = 16.2$ Hz, 1H, –CH=CH-Ph), 7.65 (dd, $J = 8.0$, 6.5 Hz, 1H, Ph C-6), 7.62–7.57 (m, 1H, 8-H), 7.52–7.47 (m, 2H, 7-H, Ph 5-H), 7.45 (d, $J = 9.8$ Hz, 1H, Ph 3-H), 7.21 (d, $J = 16.2$ Hz, 1H, -CH=CH-Ph), 1.69 (s, 6H, 1-$(CH_3)_2$). $^{13}$C NMR (176 MHz, $CDCl_3$): $\delta$ 183.6 (C-2), 163.4 (d, $^1J_{CF} = 259.1$ Hz, Ph C-2), 150.9 (C-3a), 143.4 (d, $^3J_{CF} = 7.8$ Hz, Ph C-4), 139.9 (C-9b), 133.9 (d, $^3J_{CF} = 2.5$ Hz, –CH=CH-Ph), 133.8 (Ph C-6), 132.9 (C-5a), 129.8 (C-6), 129.5 (C-5), 128.4 (C-9a), 126.6 (C-8), 125.1 (C-7), 123.8 (d, $^4J_{CF} = 3.2$ Hz, Ph C-5), 123.6 (-CH=CH-Ph), 122.9 (C-9), 120.5 (C-4), 114.4 (d, $^2J_{CF} = 20.1$ Hz, Ph C-3), 113.9 (-CN), 101.1 (d, $^2J_{CF} = 15.7$ Hz, Ph C-1), 54.5 (C-1), 22.8 (1-$(CH_3)_2$). $^{19}$F NMR (376 MHz, $CDCl_3$): $\delta$ −106.1. $^{15}$N NMR (71 MHz, $CDCl_3$): $\delta$ −66.4 (N-3), –CN not found. IR (ATR): $\nu = 2231$ (s) $cm^{-1}$ (-CN). HRMS (ESI-TOF) *m/z* $[M+H]^+$ calcd. for $C_{23}H_{18}FN_2$: 341.1449, found: 341.1446.

*4.1.2.18. 2-{(E)-2-[3,5-Bis(trifluoromethyl)phenyl]ethenyl}-1,1-dimethyl-1H-benzo[e]indole (**19**).* Compound **19** was synthesized according to the General procedure using 3,5-bis(trifluoromethyl)benzaldehyde (0.19 mL, 1.2 mmol). Yellow solid (209 mg, 48 % yield). M.p. 162–163 °C. $R_f = 0.57$ (*n*-hexane/ethyl acetate 6/1 *v/v*). $^1$H NMR (700 MHz, $CDCl_3$): $\delta$ 8.07 (d, $J = 8.4$ Hz, 1H, 9-H), 8.04 (s, 2H, Ph 2,6-H), 7.98 (d, $J = 8.2$ Hz, 1H, 6-H), 7.91 (d, $J = 8.5$ Hz, 1H, 5-H), 7.89–7.83 (m, 3H, 4-H, Ph 4-H, –CH=CH-Ph), 7.62–7.57 (m, 1H, 8-H), 7.52–7.47 (m, 1H, 7-H), 7.25 (d, $J = 16.3$ Hz, 1H, -CH=CH-Ph), 1.72 (s, 6H, 1-$(CH_3)_2$). $^{13}$C NMR (176 MHz, $CDCl_3$): $\delta$ 183.8 (C-2), 151.0 (C-3a), 139.9 (C-9b), 138.3 (Ph C-1), 133.8 (-CH=CH-Ph), 132.9 (C-5a), 132.4 (q, $^2J_{CF} = 33.2$ Hz, Ph C-3,5), 129.8 (C-6), 129.4 (C-5), 128.5 (C-9a), 127.0 (q, $^3J_{CF} = 3.7$ Hz, Ph C-2,6), 126.6 (C-8), 125.0 (C-7), 123.2 (q, $^1J_{CF} = 272.8$ Hz, -$CF_3$), 122.9 (C-9), 122.8 (-CH=CH-Ph), 122.3 (hept, $^3J_{CF} = 3.7$ Hz, Ph C-4), 120.5 (C-4), 54.5 (C-1), 22.9 (1-$(CH_3)_2$). $^{19}$F NMR (376 MHz, $CDCl_3$): $\delta$ −63.0 ($CF_3$). $^{15}$N NMR (71 MHz, $CDCl_3$): $\delta$ −67.2 (N-3). IR (ATR): $\nu = 3045$ (m), 2971 (m), 2917 (w), 2872 (w) $cm^{-1}$ ($CH_{arom}$, $CH_{aliph}$). HRMS (ESI-TOF) *m/z* $[M+H]^+$ calcd. for $C_{24}H_{18}F_6N$: 434.1338, found: 434.1336.

*4.1.2.19. 5-[(E)-2-(1,1-Dimethyl-1H-benzo[e]indol-2-yl)ethenyl]-2-fluorobenzonitrile (**20**).* Compound **20** was synthesized according to the General procedure using 3-cyano-4-fluorobenzaldehyde (224 mg, 1.5 mmol). After flash chromatography on silica gel (eluent – *n*-hexane/ethyl acetate 6/1 *v/v*), **20** was obtained as a orange amorphous material (111 mg, 33 % yield). $R_f = 0.13$ (*n*-hexane/ethyl acetate 6/1 *v/v*). $^1$H NMR (700 MHz, $CDCl_3$): $\delta$ 8.06 (d, $J = 8.3$ Hz, 1H, 9-H), 7.97 (d, $J = 8.3$ Hz, 1H, 6-H), 7.92–7.81 (m, 4H, 4,5-H, Ph 4,6-H), 7.78 (d, $J = 16.2$ Hz, 1H, –CH=CH-Ph), 7.58 (t, $J = 7.6$ Hz, 1H, 8-H), 7.48 (t, $J = 7.5$ Hz, 1H, 7-H), 7.26 (d, $J = 7.7$ Hz, 1H, Ph 3-H), 7.09 (d, $J = 16.2$ Hz, 1H, -CH=CH-Ph), 1.69 (s, 6H, 1-$(CH_3)_2$). $^{13}$C NMR (176 MHz, $CDCl_3$): $\delta$ 184.0 (C-2), 163.1 (d, $^1J_{CF} = 262.4$ Hz, Ph C-2), 150.8 (C-3a), 139.6 (C-9b), 133.69 (d, $^3J_{CF} = 6.7$ Hz, Ph C-4), 133.66 (d, $^4J_{CF} = 3.9$ Hz, Ph C-5), 133.6 (-CH=CH-Ph), 132.8 (C-5a), 132.0 (Ph C-6), 129.8 (C-6), 129.4 (C-5), 128.5 (C-9a), 126.6 (C-8), 125.0 (C-7), 122.9 (C-9), 121.1 (d, $^6J_{CF} = 2.4$ Hz, -CH=CH-Ph), 120.4 (C-4), 117.3 (d, $^2J_{CF} = 20.1$ Hz, Ph C-3), 113.6 (-CN), 102.4 (d, $^2J_{CF} = 16.2$ Hz, Ph C-1), 54.5 (C-1), 22.9 (1-$(CH_3)_2$). $^{19}$F NMR (376 MHz, $CDCl_3$): $\delta$ −105.7. $^{15}$N NMR (71 MHz, $CDCl_3$): $\delta$ −70.8 (N-3), –CN not found. IR (ATR): $\nu = 2238$ (s) $cm^{-1}$ (-CN). HRMS (ESI-TOF) *m/z* $[M+H]^+$ calcd. for $C_{23}H_{18}FN_2$: 341.1449, found: 341.1452.

*4.1.2.20. 2-[(E)-2-(2-Chloro-5-nitrophenyl)ethenyl]-1,1-dimethyl-1H-benzo[e]indole (**21**).* Compound **21** was synthesized according to the General procedure using 2-chloro-5-nitrobenzaldehyde (278 mg, 1.5 mmol). Yellow solid (289 mg, 77 % yield). M.p. 191–192 °C (decomp.). $R_f = 0.38$ (*n*-hexane/ethyl acetate 6/1 *v/v*). $^1$H NMR (700 MHz, $CDCl_3$): $\delta$ 8.65 (d, $J = 2.6$ Hz, 1H, Ph 6-H), 8.17–8.11 (m, 2H, –CH=CH-Ph, Ph 4-H), 8.09 (d, $J = 8.4$ Hz, 1H, 9-H), 7.98 (d, $J = 8.2$ Hz, 1H, 6-H), 7.91 (d, $J = 8.5$ Hz, 1H, 5-H), 7.89 (d, $J = 8.5$ Hz, 1H, 4-H), 7.62 (d, $J = 8.7$ Hz, 1H, Ph 3-H), 7.59 (t, $J = 7.6$ Hz, 1H, 8-H), 7.50 (t, $J = 7.4$ Hz, 1H, 7-H), 7.28 (d, $J = 16.3$ Hz, 1H, -CH=CH-Ph), 1.74 (s, 6H, 1-$(CH_3)_2$). $^{13}$C NMR (176 MHz, $CDCl_3$): $\delta$ 183.7 (C-2), 151.0 (C-3a), 146.9 (Ph C-5), 140.6 (Ph C-2), 140.1 (C-9b), 135.9 (Ph C-1), 132.9 (C-5a), 131.1 (Ph C-3), 130.8 (-CH=CH-Ph), 129.8 (C-6), 129.4 (C-5), 128.4 (C-9a), 126.6 (C-8), 125.1 (C-7), 124.7 (-CH=CH-Ph), 123.9 (Ph C-4), 122.9 (C-9), 121.8 (Ph C-6), 120.7, 54.6 (C-1), 23.1 (1-$(CH_3)_2$). $^{15}$N NMR (71 MHz, $CDCl_3$): $\delta$ −64.0 (N-3), −14.8 (-$NO_2$). IR (ATR): $\nu = 1519$ (vs), 1347 (s) $cm^{-1}$ (-$NO_2$). HRMS (ESI-TOF) *m/z* $[M+H]^+$ calcd. for $C_{22}H_{18}ClN_2O_2$: 377.1051, found: 377.1048.

*4.1.3. Alternative procedure for the synthesis of compounds **4,5***

1,1,2-Trimethyl-1*H*-benzo[*e*]indole **1** (1 mmol, 1 eq.) was dissolved in ethanol (2 mL), 4-(dimethylamino)benzaldehyde (for the synthesis of compound **4**) or 4-(diethylamino)benzaldehyde (for the synthesis of compound **5**) (1.5 mmol, 1.5 eq.) and trifluoroacetic acid (100 μL) were added. The reaction mixture was stirred at reflux for 24 h. Upon cooling, the solvent was removed under reduced pressure and the residue was subjected to column chromatography on silica gel.

*4.1.3.1. 4-[(E)-2-(1,1-Dimethyl-1H-benzo[e]indol-2-yl)ethenyl]-N,N-dimethylaniline (**4**), previously reported in [25].* Compound **4** was synthesized using 4-(dimethylamino)benzaldehyde (212 mg, 1.5 mmol). After flash chromatography on silica gel (eluent – *n*-hexane/ethyl acetate 6/1 v/v), **4** was obtained as a reddish-brown amorphous material (105 mg, 31 % yield).

*4.1.3.2. 4-[(E)-2-(1,1-Dimethyl-1H-benzo[e]indol-2-yl)ethenyl]-N,N-diethylaniline (**5**).* Compound **5** was synthesized using 4-(diethylamino) benzaldehyde (254 mg, 1.5 mmol). After flash chromatography on silica gel (eluent – *n*-hexane/ethyl acetate 4/1 *v/v*), **5** was obtained as a brown amorphous material (202 mg, 55 % yield).

*4.1.4. Procedure for the synthesis of compound **22***

1,1,2-Trimethyl-1*H*-benzo[*e*]indole **1** (1 mmol, 1 eq.) was dissolved in ethanol (2 mL), 4-fluoro-3-nitrobenzaldehyde (1.5 mmol, 1.5 eq.) and triethylamine (60 μL) were added. The reaction mixture was stirred at reflux for 24 h. Upon cooling, the resulting crystals were filtered, washed with ethanol, recrystallized from ethanol, and dried.

*4.1.4.1. 2-(E)-2-(4-Fluoro-3-nitrophenyl)ethenyl-1,1-dimethyl-1H-benzo[e]indole (**22**).* Yellow solid (197 mg, 55 % yield). M.p. 201–202 °C (decomp.) $R_f = 0.13$ (*n*-hexane/ethyl acetate 6/1 *v/v*). $^1$H NMR (700 MHz, $CDCl_3$): $\delta$ 8.33 (d, $J = 6.3$ Hz, 1H, Ph 2-H), 8.06 (d, $J = 8.4$ Hz, 1H, 9-H), 7.97 (d, $J = 8.1$ Hz, 1H, 6-H), 7.93–7.78 (m, 4H, 4,5-H, Ph 6-H, –CH=CH-Ph), 7.59 (t, $J = 7.6$ Hz, 1H, 8-H), 7.49 (t, $J = 7.4$ Hz, 1H, 7-H), 7.35 (t, $J = 9.4$ Hz, 1H, Ph 5-H), 7.15 (d, $J = 16.2$ Hz, 1H, -CH=CH-Ph), 1.70 (s, 6H, 1-$(CH_3)_2$). $^{13}$C NMR (176 MHz, $CDCl_3$): $\delta$ 183.9 (C-2), 155.4 (d, $^1J_{CF} = 268.0$ Hz, Ph C-4), 150.9 (C-3a), 139.7 (C-9b), 137.8 (d, $^2J_{CF} = 7.8$ Hz, Ph C-3), 134.1 (d, $^3J_{CF} = 8.4$ Hz, Ph C-6), 133.5 (d, $^4J_{CF} = 4.3$ Hz, Ph C-1), 133.4 (d, $^5J_{CF} = 1.5$ Hz, –CH=CH-Ph), 132.8 (C-5a), 129.8 (C-6), 129.4 (C-5), 128.5 (C-9a), 126.6 (C-8), 125.0 (C-7), 124.2 (d, $^3J_{CF} = 2.6$ Hz, Ph C-2), 122.9 (C-9), 121.7 (d, $^6J_{CF} = 2.4$ Hz, -CH=CH-Ph), 120.4 (C-4), 119.1 (d, $^2J_{CF} = 21.4$ Hz, Ph C-5), 54.5 (C-1), 22.8 (1-$(CH_3)_2$). $^{19}$F NMR (376 MHz, $CDCl_3$): $\delta$ −116.5. $^{15}$N NMR (71 MHz, $CDCl_3$): $\delta$ −69.7 (N-3), −18.5 (-$NO_2$). IR (ATR): $\nu = 1533$, 1348 $cm^{-1}$ (-$NO_2$). HRMS (ESI-TOF) *m/z* $[M+H]^+$ calcd. for

$C_{22}H_{18}FN_2O_2$: 361.1347, found: 361.1345.

### 4.2. Biology

#### 4.2.1. Photodynamic treatment

An in-house constructed LED based light source specifically designed for the irradiation of 96-well microplates and Petri dishes [46] was used; a maximal wavelength emission of 414 nm, light intensity set to 20 mW/cm$^2$. The total dose of irradiation did not affect the temperature during irradiation.

#### 4.2.2. Cell cultures and cytotoxicity assays

G361 and A375-derived ARN8 human melanoma cells and BJ human nontransformed foreskin fibroblasts were cultivated in DMEM medium without phenol red supplemented with 10 % fetal bovine serum, penicillin (100 U/mL) and streptomycin (100 μg/mL) at 37 °C in 5 % $CO_2$ atmosphere.

Cytotoxicity was determined using the MTT (Sigma-Aldrich, St. Louis, MO, USA) assay in 96-well microplates. The test compounds were added 24 h post plating, the cells were then incubated for additional 4 h and irradiated (the maximal wavelength emission of 414 nm and total dose of 2.5, 5 or 10 J/cm$^2$). After irradiation, the cells were incubated for further 20 h or 68 h and then the MTT solution was added, cells were incubated for another 4 h at 37 °C and in 5 % $CO_2$ and then the 10 % SDS was added to the wells to solubilize the violet formazan crystals. The measurement of absorbance was carried out on reader Tecan Infinite M200Pro (Tecan, Männedorf, Switzerland) at 570 nm. Dark viability was measured in parallel under the same conditions without irradiation.

#### 4.2.3. ROS detection

The ROS production measurement using CM-$H_2$DCFDA (Invitrogen, Waltham, MA, USA) fluorescent probe was performed according to manufacturer's guidelines. Briefly, the cells were plated and next day labeled with the 5 μM probe (30 min loading time), loading buffer was removed and replaced with prewarmed PBS with 5 mM glucose and for 4 h treated with test compound. After irradiation (5 and 10 J/cm$^2$), the ROS levels were measured immediately on Tecan Infinite M200Pro (Tecan, Männedorf, Switzerland) at 492/530 nm (ex/em). Negative control samples were established by 10 min pretreatment with *N*-acetylcysteine (5 mM), inhibitor of ROS. Evaluation of oxidative stress using DHR123 (Enzo, Farmingdale, NY, USA), HPF (Enzo, Farmingdale, NY, USA) and SOSG (Invitrogen, Waltham, MA, USA) probes was performed in G361 and ARN8 cells. Briefly, the cells were plated and next day treated with test compound. After 4 h incubation, the medium with test compound was replaced with PBS containing 5 μM probe for 30 min. Subsequently, the labelling solution was discarded, cells in PBS were irradiated (5 and 10 J/cm$^2$) and the ROS levels were measured immediately on Tecan Infinite M200Pro (Tecan, Männedorf, Switzerland) at 490/525 nm (ex/em). ROS production in samples kept in the dark was always measured in parallel under the same conditions without irradiation.

Water solutions of **15** were mixed with DHR123, SOSG or HPF probes at final concentration of 5 μM and measured immediately after irradiation with blue light (10 J/cm$^2$) on Tecan Infinite M200Pro (Tecan, Männedorf, Switzerland) at 490/525 nm (ex/em).

#### 4.2.4. Immunoblotting

Cell lysates were prepared in RIPA buffer. Proteins were separated on SDS-polyacrylamide gels, electroblotted onto nitrocellulose membranes and after blocking, overnight incubation with specific primary antibodies and incubation with peroxidase-conjugated secondary antibodies, the peroxidase activity was detected with SuperSignal West Pico reagents (Thermo Scientific) using a CCD camera LAS-4000 (Fujifilm, Tokyo, Japan). All primary antibodies were diluted in TBS containing 4 % BSA and 0.1 % Tween 20. The specific antibodies were purchased from Cell Signaling, Danvers, MA, USA (anti-PARP-1, clone 46D11; anti-BAX, clone D2E11; anti-Mcl-1, clone D35A5; anti-caspase 9; anti-caspase 7; anti-HO-1, clone E7U4W), Sigma-Aldrich, St. Louis, MO, USA (anti-Bcl-2), Merck Millipore, Burlington, MA, USA (anti-phosphohistone H2A.X, Ser139, clone JBW301) and Santa Cruz Biotechnology, Dallas, TX, USA (anti-GAPDH, clone 0411). Anti-p53, clone DO-1 was generously gifted by dr. B. Vojtěšek (Masaryk Memorial Cancer Institute, Brno).

#### 4.2.5. Cell cycle analysis

Cells were seeded, after a preincubation period, treated with tested compound for 4 h, irradiated, and subsequently incubated for further 20 h. After staining with propidium iodide, DNA content was analyzed by flow cytometry using a 488 nm laser (BD FACSVerse with BD FACSuite software, version 1.0.6; BD, Franklin Lakes, NJ, USA). Cell cycle distribution was analyzed using ModFit LT (Verity Software House).

#### 4.2.6. Comet assay

G361 cells were trypsinized, rinsed by DMEM and then the cell suspension in 1 % LMP agarose was pipetted to the microscope slides with agarose gel. The microscope slides were immersed in a lysis buffer with 1 % Triton X for 1 h and then placed in an electrophoretic tank and dipped into a cool electrophoresis solution for 40 min. After the electrophoresis (20 V, 350 mA, 20 min), the microscopic slides were immersed in a neutralisation buffer (10 min twice). The samples were then stained by SYBR Green (Invitrogen, Waltham, MA, USA) for 15 min and scored by the SW Comet Score (TriTek Corp., Wilmington, DE, USA).

#### 4.2.7. p53 reporter assay

The p53-dependent transcriptional activity was determined using β-galactosidase reporter assay in ARN8 stably transfected with a p53-responsive reporter construct pRGCΔfoslacZ. Cells were treated with increasing concentrations of tested compound and after 4 h incubation, irradiated with blue light (414 nm; 2.5, 5, 7.5 and 10 J/cm$^2$) and incubated for further 20 h. The cells were then lysed using 0.3 % Triton X-100 and after 10 min, the substrate 4-methylumbelliferyl β-D-galactopyranoside at a final concentration of 80 μM was added for 1 h. The fluorescence was measured at 355/360 nm (ex/em) with a Fluoroskan Ascent microplate reader (Labsystems, Vantaa, Finland).

## CRediT authorship contribution statement

**Gabrielė Varvuolytė:** Writing – original draft, Investigation, Formal analysis. **Eva Řezníčková:** Writing – original draft, Investigation, Formal analysis. **Sonata Krikštolė:** Investigation. **Rasa Tamulienė:** Investigation. **Aurimas Bieliauskas:** Writing – review & editing, Formal analysis, Data curation. **Lukáš Malina:** Investigation. **Veronika Vojáčková:** Investigation. **Zdenko Duben:** Investigation. **Hana Kolářová:** Resources, Methodology. **Neringa Kleizienė:** Writing – review & editing, Supervision. **Eglė Arbačiauskienė:** Writing – review & editing, Project administration. **Asta Žukauskaitė:** Writing – review & editing. **Vladimír Kryštof:** Writing – review & editing, Resources, Funding acquisition, Data curation, Conceptualization. **Algirdas Šačkus:** Writing – review & editing, Resources, Funding acquisition, Conceptualization.

## Declaration of competing interest

The authors declare the following financial interests/personal relationships which may be considered as potential competing interests:

A patent application titled '1,1-Dimethyl-2-[(E)-2-Phenylethenyl]-1H-benzo[e]indole Derivatives and Uses Thereof' (U.S. App. 18/456,145) has been filed by Gabriele Varvuolyte, Eva Reznickova, Sonata Krikstolaityte (currently - Sonata Krikstole), Aurimas Bieliauskas, Veronika Vojackova, Neringa Kleiziene, Egle Arbaciauskiene, Asta Zukauskaite, Vladimir Krystof and Algirdas Sackus. Any additional authors declare that they have no known competing financial interests or

personal relationships that could have influenced the work reported in this paper.

## Data availability

Data will be made available on request.

## Acknowledgements

This work was supported by the Research Council of Lithuania (No. S-MIP-23-51), the European Union - Next Generation EU (The project National Institute for Cancer Research, Programme EXCELES, Project No. LX22NPO5102), the Doctoral Fund of Kaunas University of Technology (No. A-410, approved June 26, 2019) and the Internal Grant Agency of Palacký University Olomouc (IGA_PrF_2024_005). The authors would like to thank Anna Krnáčová for excellent technical assistance. Anti-p53, clone DO-1 was generously gifted by dr. B. Vojtěšek (Masaryk Memorial Cancer Institute, Brno).

## Appendix A. Supplementary data

Supplementary data to this article can be found online at https://doi.org/10.1016/j.ejmech.2024.116777.

## References

[1] S.H. Sinha, E.A. Owens, Y. Feng, Y. Yang, Y. Xie, Y. Tu, M. Henary, Y.G. Zheng, Synthesis and evaluation of carbocyanine dyes as PRMT inhibitors and imaging agents, Eur. J. Med. Chem. 54 (2012) 647–659, https://doi.org/10.1016/j.ejmech.2012.06.017.

[2] Y. Chen, J. Wu, L. Yang, B. Hu, D. Yang, Z. Lu, Y. Huang, Synthesis of 3*H*-Benzo[e]indoline and Its Application to Small-Molecule Organic Solar Cells, Chem. Eur J. 24 (2018) 8747–8750, https://doi.org/10.1002/chem.201800938.

[3] A. Abdollahi, H. Roghani-Mamaqani, M. Salami-Kalajahi, B. Razavi, K. Sahandi-Zangabad, Encryption and optical authentication of confidential cellulosic papers by ecofriendly multi-color photoluminescent inks, Carbohydr. Polym. 245 (2020) 116507, https://doi.org/10.1016/j.carbpol.2020.116507.

[4] S. Samanta, S. Halder, G. Das, Twisted-intramolecular-charge-transfer-based turn-on fluorogenic nanoprobe for real-time detection of serum albumin in physiological conditions, Anal. Chem. 90 (2018) 7561–7568, https://doi.org/10.1021/acs.analchem.8b01181.

[5] Y. Sun, S. Fan, D. Zhao, L. Duan, R. Li, A fluorescent turn-on probe based on benzo [*E*] indolium for cyanide ion in water with high selectivity, J. Fluoresc. 23 (2013) 1255–1261, https://doi.org/10.1007/s10895-013-1258-y.

[6] S. Samanta, P. Dey, A. Ramesh, G. Das, A solo fluorogenic probe for the real-time sensing of $SO_3^{2-}$ and $SO_4^{2-}$/$HSO_4^-$ in aqueous medium and live cells by distinct turn-on emission signals, Chem. Commun. 52 (2016) 10381–10384, https://doi.org/10.1039/C6CC03910C.

[7] B. Huang, W. Chen, Y.-Q. Kuang, W. Liu, X.-J. Liu, L.-J. Tang, J.-H. Jiang, A novel off–on fluorescent probe for sensitive imaging of mitochondria-specific nitroreductase activity in living tumor cells, Org. Biomol. Chem. 15 (2017) 4383–4389, https://doi.org/10.1039/C7OB00781G.

[8] B. Chen, C. Li, J. Zhang, J. Kan, T. Jiang, J. Zhou, H. Ma, Sensing and imaging of mitochondrial viscosity in living cells using a red fluorescent probe with a long lifetime, Chem. Commun. 55 (2019) 7410–7413, https://doi.org/10.1039/C9CC03977E.

[9] C. Han, H. Yang, M. Chen, Q. Su, W. Feng, F. Li, Mitochondria-Targeted near-infrared fluorescent off–on probe for selective detection of cysteine in living cells and *in vivo*, ACS Appl. Mater. Interfaces 7 (2015) 27968–27975, https://doi.org/10.1021/acsami.5b10607.

[10] Y. Liu, K. Li, K.-X. Xie, L.-L. Li, K.-K. Yu, X. Wang, X.-Q. Yu, A water-soluble and fast-response mitochondria-targeted fluorescent probe for colorimetric and ratiometric sensing of endogenously generated $SO_2$ derivatives in living cells, Chem. Commun. 52 (2016) 3430–3433, https://doi.org/10.1039/C5CC10505F.

[11] G. Yin, Y. Gan, T. Yu, T. Niu, P. Yin, H. Chen, Y. Zhang, H. Li, S. Yao, A dual-emission and mitochondria-targeted fluorescent probe for rapid detection of $SO_2$ derivatives and its imaging in living cells, Talanta 191 (2019) 428–434, https://doi.org/10.1016/j.talanta.2018.08.059.

[12] J. Xu, H. Yuan, C. Qin, L. Zeng, G.-M. Bao, A mitochondria-targeted near-infrared probe for colorimetric and ratiometric fluorescence detection of hypochlorite in living cells, RSC Adv. 6 (2016) 107525–107532, https://doi.org/10.1039/C6RA22868B.

[13] X. Chen, W. Peng, S. Huang, C. Yang, M. Hu, S. Yang, S. Yang, Y. Xie, H. Chen, N. Lei, Y. Luo, K. Li, Novel mitochondria-targeted and fluorescent DNA alkylation agents with highly selective activity against cancer cells, Dyes Pigm. 170 (2019) 107610, https://doi.org/10.1016/j.dyepig.2019.107610.

[14] S.M. Mahalingam, J.D. Ordaz, P.S. Low, Targeting of a photosensitizer to the mitochondrion enhances the potency of photodynamic therapy, ACS Omega 3 (2018) 6066–6074, https://doi.org/10.1021/acsomega.8b00692.

[15] H.-J. Lim, C.-H. Oh, Indocyanine green-based photodynamic therapy with 785nm light emitting diode for oral squamous cancer cells, Photodiagnosis Photodyn. Ther. 8 (2011) 337–342, https://doi.org/10.1016/j.pdpdt.2011.06.002.

[16] C. Shirata, J. Kaneko, Y. Inagaki, T. Kokudo, M. Sato, S. Kiritani, N. Akamatsu, J. Arita, Y. Sakamoto, K. Hasegawa, N. Kokudo, Near-infrared photothermal/photodynamic therapy with indocyanine green induces apoptosis of hepatocellular carcinoma cells through oxidative stress, Sci. Rep. 7 (2017) 13958, https://doi.org/10.1038/s41598-017-14401-0.

[17] H. Gu, W. Liu, W. Sun, J. Du, J. Fan, X. Peng, Single-molecule photosensitizers for NIR-II fluorescence and photoacoustic imaging guided precise anticancer phototherapy, Chem. Sci. 13 (2022) 9719–9726, https://doi.org/10.1039/D2SC02879D.

[18] W. Zhu, M. Kang, Q. Wu, Z. Zhang, Y. Wu, C. Li, K. Li, L. Wang, D. Wang, B.Z. Tang, Zwitterionic AIEgens: rational molecular design for NIR-II fluorescence imaging-guided synergistic phototherapy, Adv. Funct. Mater. 31 (2021) 2007026, https://doi.org/10.1002/adfm.202007026.

[19] D.M. Dereje, C. Pontremoli, M.J. Moran Plata, S. Visentin, N. Barbero, Polymethine dyes for PDT: recent advances and perspectives to drive future applications, Photochem. Photobiol. Sci. 21 (2022) 397–419, https://doi.org/10.1007/s43630-022-00175-6.

[20] R. Tian, C. Wang, W. Chi, J. Fan, J. Du, S. Long, L. Guo, X. Liu, X. Peng, Emerging design principle of near-infrared upconversion sensitizer based on mitochondria-targeted organic dye for enhanced photodynamic therapy, Chem. Eur J. 27 (2021) 16707–16715, https://doi.org/10.1002/chem.202102866.

[21] L. Fan, Y.-J. Fu, Q.-L. Liu, D.-T. Lu, C. Dong, S.-M. Shuang, Novel far-visible and near-infrared pH probes based on styrylcyanine for imaging intracellular pH in live cells, Chem. Commun. 48 (2012) 11202, https://doi.org/10.1039/c2cc35363f.

[22] Y. Zhang, Y. Zhao, Y. Wu, B. Zhao, L. Wang, B. Song, C. Huang, Benzoindole-based bifunctional ratiometric turn-on sensor with an ICT effect for trapping of $H^+$ and $Al^{3+}$ in dual-channel cell imaging and samples, Spectrochim. Acta Mol. Biomol. Spectrosc. 247 (2021) 119123, https://doi.org/10.1016/j.saa.2020.119123.

[23] W. Niu, M. Nan, L. Fan, M.S. Wong, S. Shuang, C. Dong, A novel pH fluorescent probe based on indocyanine for imaging of living cells, Dyes Pigm. 126 (2016) 224–231, https://doi.org/10.1016/j.dyepig.2015.11.027.

[24] L. Fan, S.-Q. Gao, Z.-B. Li, W.-F. Niu, W.-J. Zhang, S.-M. Shuang, C. Dong, An indole-carbazole-based ratiometric emission pH fluorescent probe for imaging extreme acidity, Sens Actuators B Chem 221 (2015) 1069–1076, https://doi.org/10.1016/j.snb.2015.07.076.

[25] Y. Zhang, Y. Zhao, Y. Wu, B. Zhao, L. Wang, B. Song, Hemicyanine based naked-eye ratiometric fluorescent probe for monitoring lysosomal pH and its application, Spectrochim. Acta Mol. Biomol. Spectrosc. 227 (2020) 117767, https://doi.org/10.1016/j.saa.2019.117767.

[26] D. Zhang, S. Wang, F. Yang, Q. Qi, Y. Li, W. Huang, A fluorescent probe for alkylating agents and its quantification of triflate as a genotoxic impurity, Chem. Commun. 59 (2023) 2130–2133, https://doi.org/10.1039/D2CC06221F.

[27] K. van Beurden, S. de Koning, D. Molendijk, J. van Schijndel, The Knoevenagel reaction: a review of the unfinished treasure map to forming carbon–carbon bonds, Green Chem. Lett. Rev. 13 (2020) 349–364, https://doi.org/10.1080/17518253.2020.1851398.

[28] S. Jiao, S. Yang, X. Meng, C. Wang, One step synthesis of red-emitting fluorescence turn-on probe for nitroreductase and its application to bacterial detection and oral cancer cell imaging, Spectrochim. Acta Mol. Biomol. Spectrosc. 241 (2020) 118637, https://doi.org/10.1016/j.saa.2020.118637.

[29] Q. Bai, C. Yang, M. Yang, Z. Pei, X. Zhou, J. Liu, H. Ji, G. Li, M. Wu, Y. Qin, Q. Wang, L. Wu, pH-dominated selective imaging of lipid droplets and mitochondria via a polarity-reversible ratiometric fluorescent probe, Anal. Chem. 94 (2022) 2901–2911, https://doi.org/10.1021/acs.analchem.1c04806.

[30] J. Zhou, S. Xu, X. Dong, W. Zhao, Q. Zhu, 3,5-dinitropyridin-2-yl as a fast thiol-responsive capping moiety in the development of fluorescent probes of biothiols, Dyes Pigm. 167 (2019) 157–163, https://doi.org/10.1016/j.dyepig.2019.04.020.

[31] C. Gao, Y. Tian, R. Zhang, J. Jing, X. Zhang, Mitochondrial directed ratiometric fluorescent probe for quantitive detection of sulfur dioxide derivatives, New J. Chem. 43 (2019) 5255–5259, https://doi.org/10.1039/C8NJ05951A.

[32] S. Roberts, M. Seeger, Y. Jiang, A. Mishra, F. Sigmund, A. Stelzl, A. Lauri, P. Symvoulidis, H. Rolbieski, M. Preller, X.L. Deán-Ben, D. Razansky, T. Orschmann, S.C. Desbordes, P. Vetschera, T. Bach, V. Ntziachristos, G. G. Westmeyer, Calcium sensor for photoacoustic imaging, J. Am. Chem. Soc. 140 (2018) 2718–2721, https://doi.org/10.1021/jacs.7b03064.

[33] W. Shen, G. Hu, H. Xu, W. Sun, Y. Hu, W. Yang, Construction and evaluation of ratiometric fluorescent probes based on a 7-aminocoumarin scaffold for the detection of $SO_2$ derivatives, Dyes Pigm. 198 (2022) 109971, https://doi.org/10.1016/j.dyepig.2021.109971.

[34] A. Perry, New mechanism, new chromophore: investigating the electrophilic behaviour of styrylindolium dyes, Org. Biomol. Chem. 17 (2019) 4825–4834, https://doi.org/10.1039/C9OB00641A.

[35] M. Bokan, K. Bondar, V. Marks, G. Gellerman, L.D. Patsenker, Switchable phenolocyanine reporters containing reactive alkylcarboxylic groups for fluorescence-based targeted drug delivery monitoring, Dyes Pigm. 159 (2018) 18–27, https://doi.org/10.1016/j.dyepig.2018.05.046.

[36] J. Cheng, Z. Li, W. Lin, Development of a one-step synthesized red emission fluorescent probe for sensitive detection of viscosity in vitro and in vivo, Spectrochim. Acta Mol. Biomol. Spectrosc. 258 (2021) 119808, https://doi.org/10.1016/j.saa.2021.119808.

[37] S.Y. Park, K. Kim, D.-H. Cho, E.-Y. Jo, C. Kang, M.H. Lee, An indole-based fluorescent chemosensor targeting the autophagosome, Chem. Commun. 58 (2022) 2886–2889, https://doi.org/10.1039/D1CC06681A.
[38] H. Wang, M. Dong, H. Wang, F. Huang, P. Li, W. Zhang, W. Zhang, B. Tang, Ultrasensitive and ratiometric two-photon fluorescence imaging of Golgi polarity during drug-induced acute kidney injury, Chem. Commun. 57 (2021) 5838–5841, https://doi.org/10.1039/D1CC01411K.
[39] S. Rohrbach, A.J. Smith, J.H. Pang, D.L. Poole, T. Tuttle, S. Chiba, J.A. Murphy, Concerted nucleophilic aromatic substitution reactions, Angew. Chem. Int. Ed. 58 (2019) 16368–16388, https://doi.org/10.1002/anie.201902216.
[40] W.R. Dolbier, in: Guide to Fluorine NMR for Organic Chemists, second ed., John Wiley & Sons, Inc., 2016.
[41] M. Chen, D. Chen, P. Chou, Fluorescent chromophores containing the nitro group: relatively unexplored emissive properties, ChemPlusChem 86 (2021) 11–27, https://doi.org/10.1002/cplu.202000592.
[42] C.-X. Zhao, T. Liu, M. Xu, H. Lin, C.-J. Zhang, A fundamental study on the fluorescence-quenching effect of nitro groups in tetraphenylethene AIE dyes with electron-withdrawing groups, Chin. Chem. Lett. 32 (2021) 1925–1928, https://doi.org/10.1016/j.cclet.2021.02.008.
[43] Y.M. Poronik, G.V. Baryshnikov, I. Deperasińska, E.M. Espinoza, J.A. Clark, H. Ågren, D.T. Gryko, V.I. Vullev, Deciphering the unusual fluorescence in weakly coupled bis-nitro-pyrrolo[3,2-*b*]pyrroles, Commun. Chem. 3 (2020) 190, https://doi.org/10.1038/s42004-020-00434-6.
[44] Y.M. Poronik, B. Sadowski, K. Szychta, F.H. Quina, V.I. Vullev, D.T. Gryko, Revisiting the non-fluorescence of nitroaromatics: presumption *versus* reality, J. Mater. Chem. C Mater 10 (2022) 2870–2904, https://doi.org/10.1039/D1TC05423F.
[45] S. Kwiatkowski, B. Knap, D. Przystupski, J. Saczko, E. Kędzierska, K. Knap-Czop, J. Kotlińska, O. Michel, K. Kotowski, J. Kulbacka, Photodynamic therapy – mechanisms, photosensitizers and combinations, Biomed. Pharmacother. 106 (2018) 1098–1107, https://doi.org/10.1016/j.biopha.2018.07.049.
[46] R. Bajgar, H. Kolarova, P. Kolar, K. Pizova, A. Hanakova, Light Source Intended Particulary for in Vitro Creating and Monitoring Photodynamic Phenomena (CZ28377U1), 2015.
[47] B. Razmienė, V. Vojáčková, E. Řezníčková, L. Malina, V. Dambrauskienė, M. Kubala, R. Bajgar, H. Kolářová, A. Žukauskaitė, E. Arbačiauskienė, A. Šačkus, V. Kryštof, Synthesis of *N*-aryl-2,6-diphenyl-2*H*-pyrazolo[4,3-*c*]pyridin-7-amines and their photodynamic properties in the human skin melanoma cell line G361, Bioorg. Chem. 119 (2022) 105570, https://doi.org/10.1016/j.bioorg.2021.105570.
[48] Z. Zhou, J. Song, L. Nie, X. Chen, Reactive oxygen species generating systems meeting challenges of photodynamic cancer therapy, Chem. Soc. Rev. 45 (2016) 6597–6626, https://doi.org/10.1039/C6CS00271D.
[49] G. Varvuolytė, E. Řezníčková, A. Bieliauskas, N. Kleizienė, V. Vojáčková, A. Opichalová, A. Žukauskaitė, V. Kryštof, A. Šačkus, Synthesis and photodynamic activity of new 5-[(*E*)-2-(3-alkoxy-1-phenyl-1*H*-pyrazol-4-yl)ethenyl]-2-phenyl-3*H*-indoles, Arch. Pharm. (Weinheim) (2024), https://doi.org/10.1002/ardp.202400282.
[50] A.P. Thomas, P.S. Saneesh Babu, S. Asha Nair, S. Ramakrishnan, D. Ramaiah, T. K. Chandrashekar, A. Srinivasan, M. Radhakrishna Pillai, *meso*-Tetrakis(*p*-sulfonatophenyl)N-Confused porphyrin tetrasodium salt: a potential sensitizer for photodynamic therapy, J. Med. Chem. 55 (2012) 5110–5120, https://doi.org/10.1021/jm300009q.
[51] L. Žárská, Z. Malá, K. Langová, L. Malina, S. Binder, R. Bajgar, H. Kolářová, The effect of two porphyrine photosensitizers TMPyP and ZnTPPS4 for application in photodynamic therapy of cancer cells in vitro, Photodiagnosis Photodyn. Ther. 34 (2021) 102224, https://doi.org/10.1016/j.pdpdt.2021.102224.
[52] M.S. Baptista, J. Cadet, P. Di Mascio, A.A. Ghogare, A. Greer, M.R. Hamblin, C. Lorente, S.C. Nunez, M.S. Ribeiro, A.H. Thomas, M. Vignoni, T.M. Yoshimura, Type I and type II photosensitized oxidation reactions: guidelines and mechanistic pathways, Photochem. Photobiol. 93 (2017) 912–919, https://doi.org/10.1111/php.12716.
[53] W. Udomsak, M. Kucinska, J. Pospieszna, H. Dams-Kozlowska, W. Chatuphonprasert, M. Murias, Antioxidant enzymes in cancer cells: their role in photodynamic therapy resistance and potential as targets for improved treatment outcomes, Int. J. Mol. Sci. 25 (2024) 3164, https://doi.org/10.3390/ijms25063164.
[54] D. Nowis, M. Legat, T. Grzela, J. Niderla, E. Wilczek, G.M. Wilczynski, E. Głodkowska, P. Mrówka, T. Issat, J. Dulak, A. Józkowicz, H. Waś, M. Adamek, A. Wrzosek, S. Nazarewski, M. Makowski, T. Stokłosa, M. Jakóbisiak, J. Gołab, Heme oxygenase-1 protects tumor cells against photodynamic therapy-mediated cytotoxicity, Oncogene 25 (2006) 3365–3374, https://doi.org/10.1038/sj.onc.1209378.
[55] T. Takahashi, S. Misawa, S. Suzuki, N. Saeki, Y. Shinoda, Y. Tsuneoka, J. Akimoto, Y. Fujiwara, Possible mechanism of heme oxygenase-1 expression in rat malignant meningioma KMY-J cells subjected to talaporfin sodium-mediated photodynamic therapy, Photodiagnosis Photodyn. Ther. 32 (2020) 102009, https://doi.org/10.1016/j.pdpdt.2020.102009.
[56] I. Postiglione, F. Barra, S.M. Aloj, G. Palumbo, Photodynamic therapy with 5-aminolaevulinic acid and DNA damage: unravelling roles of p53 and ABCG2, Cell Prolif. 49 (2016) 523–538, https://doi.org/10.1111/cpr.12274.
[57] J. Zawacka-Pankau, J. Krachulec, I. Grulkowski, K.P. Bielawski, G. Selivanova, The p53-mediated cytotoxicity of photodynamic therapy of cancer: recent advances, Toxicol. Appl. Pharmacol. 232 (2008) 487–497, https://doi.org/10.1016/j.taap.2008.07.012.
[58] X. Liu, X. Feng, L. Wang, D. He, H. Wen, Indocyanine Derivative and Preparation and Application Thereof (CN115557878A), 2023.